Chemical Engineering Science 227 (2020) 115863

Contents lists available at ScienceDirect

Chemical Engineering Science

journal homepage: www.elsevier.com/locate/ces

An overview on the role of lanthanide series (rare earth metals) in H_2 and syngas production from CH_4 reforming processes

Osarieme Uyi Osazuwa [a,c], Sumaiya Zainal Abidin [a,b,*]

[a] Faculty of Chemical and Process Engineering Technology, College of Engineering Technology, Universiti Malaysia Pahang, 26300 Gambang, Kuantan, Pahang, Malaysia
[b] Centre of Excellence for Advanced Research in Fluid Flow (CARIFF), Universiti Malaysia Pahang, Lebuhraya Tun Razak, 25000 Gambang, Kuantan, Pahang, Malaysia
[c] Department of Chemical Engineering, University of Benin, PMB 1154, Benin City, Edo State, Nigeria

HIGHLIGHTS

- The role of lanthanide series as catalyst, promoter and support.
- Properties affected by addition of lanthanide series to a metallic catalyst.
- Eliminating carbon from CH_4 reforming processes.
- Detailed reviews on the effects of lanthanide series on CH_4 reforming processes.

GRAPHICAL ABSTRACT

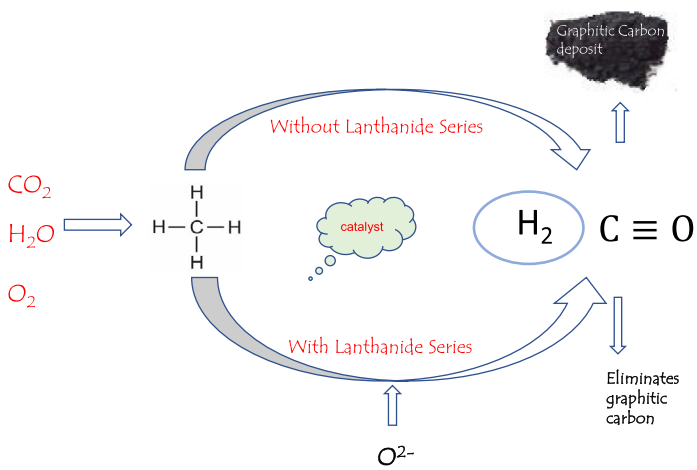

ARTICLE INFO

Article history:
Received 23 March 2020
Received in revised form 18 May 2020
Accepted 31 May 2020
Available online 6 June 2020

Keywords:
Reforming processes
Methane reforming
carbon (IV) oxide reforming
Lanthanide series
Carbon elimination

ABSTRACT

The activity of catalysts in reforming processes is greatly hindered by carbon deposition on their active sites. In this vein, a number of studies on catalyst behavior in CH_4 reforming processes have been reviewed with focus on lanthanide series as catalyst, promoter and support to improve activity and eliminate carbon. Studies have shown that various catalyst combined with the lanthanide series have effectively removed carbon from active metals sites. Therefore, this study has provided a detailed review of several works on reforming processes that have applied lanthanide series as catalyst, promoter and support. Comparative data for various CH_4 reforming processes using lanthanide series as catalyst material have been outlined. Data from this study can be applied industrially to synthesize a catalyst resistant to deactivation, hence, optimizing energy production and profit.

© 2020 Elsevier Ltd. All rights reserved.

1. Introduction

Fuel from Fossils is a major source of energy; hence, it plays a major role in the day to day activities of man. Due to constant exploration and refining, the depletion of fossil fuel is inevitable. Therefore, there is a need for alternative feed stocks for clean fuel

* Corresponding author.
E-mail address: sumaiya@ump.edu.my (S.Z. Abidin).

https://doi.org/10.1016/j.ces.2020.115863
0009-2509/© 2020 Elsevier Ltd. All rights reserved.

and chemical production (Naidja et al., 2003). Studies using alternative feed stocks have been carried out for glycerol (Veiga et al., 2019), (Mohd Arif et al., 2019), (Bobadilla et al., 2015), ethanol (Muñoz et al., 2013), (Da Silva et al., 2011), (Calles et al., 2009), propane (Azizzadeh Fard et al., 2019), (Im et al., 2018), (Natesakhawat et al., 2005), butane (Schädel et al., 2009), iso octane (Al-Musa et al., 2014) and natural gas/CH_4 (Osazuwa et al., 2018), (Horlyck et al., 2018), (Han et al., 2017).

In another perspective, there is also the need to utilize biogas from the decomposition of organic materials anaerobically. This source of fuel has been reported to possess both carbon dioxide (CO_2) and methane (CH_4) which are the main components of greenhouse gas (Izquierdo et al., 2013). So therefore, since CH_4 is the main constituent of natural gas from fossil fuel reserves, (Iyer et al., 2004) and biogas (Kohn et al., 2010), (Barrai et al., 2007), respectively, the reforming of CH_4 to more valuable products through various processes cannot be over emphasized in the present day and nearest future. Various technologies for CH_4 reforming exist and have been reported. Amongst these techniques reported include; CO_2 (Osazuwa et al., 2018a, 2018b), (Osazuwa and Cheng, 2018), steam (H_2O) (Noh et al., 2019), partial oxidation (La Parola et al., 2018), and autothermal (ARM), (Ni et al, 2014a), (Zahedinezhad et al., 2009), (Choudhary et al., 1995). In addition, some researchers have tried to reform CH_4 by using a combination of H_2O, CO_2 and O_2 as reactants. This process is termed mixed or tri-reforming of CH_4 (TRM) (Anchieta et al., 2019), (Song and Pan, 2004). Tri-reforming process is employed so as to vary the product ratio of the reaction by altering the ratio of H_2O, CO_2 and O_2. There is also the bi reforming process (Siang et al., 2019), (Singh et al., 2018) which uses the combination of two reactants; CO_2 and H_2O to shift the selectivity towards a particular product like H_2 or minimize the amount of produced carbon from the CH_4 reforming process. The basic difference between the combined reactants' reactions are the oxidant employed, product ratio obtained (M. Gaddalla and E. Sommer, 1989) and reaction kinetics or mechanism of the reaction.

The reaction pathways for the various reforming processes are represented in Eqns. (1) – (6).

CO_2 reforming of CH_4 (Buelens et al., 2016), (Pakhare and Spivey, 2014).

$$CH_4 + CO_2 \leftrightarrows 2CO + 2H_2 \left(\Delta H_{298K} = +247 kJmol^{-1}\right) \quad (1)$$

Partial oxidation of CH_4 (Pakhare and Spivey, 2014).

$$CH_4 + \frac{1}{2}O_2 \leftrightarrows CO + 2H_2 \left(\Delta H_{298K} = -36 kJmol^{-1}\right) \quad (2)$$

$$CH_4 + 2O_2 \leftrightarrows CO_2 + 2H_2O \left(\Delta H_{298K} = -803 kJmol^{-1}\right) \quad (3)$$

Steam reforming of CH_4 (Kechagiopoulos et al., 2017), (Dittmar et al., 2013).

$$CH_4 + H_2O \leftrightarrows CO + 3H_2 \left(\Delta H_{298K} = +206.2 kJmol^{-1}\right) \quad (4)$$

$$CO + H_2O \leftrightarrows CO_2 + H_2 \left(\Delta H_{298K} = -41 kJmol^{-1}\right) \quad (5)$$

$$CH_4 + 2H_2O \leftrightarrows CO_2 + 4H_2 \left(\Delta H_{298K} = 164.9 kJmol^{-1}\right) \quad (6)$$

Tri-reforming of CH_4 (Zhao et al., 2018)

$$CH_4 + CO_2 \leftrightarrows 2CO + 2H_2 \left(\Delta H_{298K} = +247 kJmol^{-1}\right) \quad (1)$$

$$CH_4 + \frac{1}{2}O_2 \leftrightarrows CO + 2H_2 \left(\Delta H_{298K} = -36 kJmol^{-1}\right) \quad (2)$$

$$CH_4 + H_2O \leftrightarrows CO + 3H_2 \left(\Delta H_{298K} = +206.2 kJmol^{-1}\right) \quad (4)$$

Autothermal reforming (Kohn et al., 2010).

$$CH_4 + CO_2 \leftrightarrows 2CO + 2H_2 \left(\Delta H_{298K} = +247 kJmol^{-1}\right) \quad (1)$$

$$CH_4 + \frac{1}{2}O_2 \leftrightarrows CO + 2H_2 \left(\Delta H_{298K} = -36 kJmol^{-1}\right) \quad (2)$$

$$CH_4 + 2O_2 \leftrightarrows CO_2 + 2H_2O \left(\Delta H_{298K} = -803 kJmol^{-1}\right) \quad (3)$$

$$CH_4 + H_2O \leftrightarrows CO + 3H_2 \left(\Delta H_{298K} = +206.2 kJmol^{-1}\right) \quad (4)$$

$$CO + H_2O \leftrightarrows CO_2 + H_2 \left(\Delta H_{298K} = -41 kJmol^{-1}\right) \quad (5)$$

Comparing the reforming processes, CO_2 reforming of CH_4 (CRM) seems to have gained more interest because of its economic value (20% more efficient economically), even though it comes with its own shortfalls which is severe carbon formation which results in catalyst deactivation (Pakhare and Spivey, 2014). CRM proceeds as an endothermic catalytic process which yields approximately unity syngas ratio and traces of CO_2 (Bitter et al., 2000), (Galuszka et al., 1998). Application of this process is seen in the solar-chemical energy transmission plants (Araujo et al., 2008), (G. S. Gallego et al., 2008), where the heat energy from the sun is directed to power the process because of the endothermicity of the main reaction. Another advantage of the CRM process is the utilization of two greenhouse gases which are abundantly present in the atmosphere. These gases are converted to H_2 and CO with ratio of about unity. This type of product (H_2 and CO) is required as feedstock for industrialized processes like the Fischer-Tropsch process. For the steam reforming process, which has been highly commercialized for the production of H_2, a significant amount of carbon and CO_2 is also produced. Removal of these undesired products adds additional cost to the process, thereby becoming a challenge in the petrochemical industry (Ross, 2005). More significantly, the syngas ratio in the steam reforming process is high, hence, making the process suitable for H_2 production but unsuitable for synthesis of liquid hydrocarbon and methanol which require lower syngas ratio (Gronchi et al., 1997). For the partial oxidation of CH_4, resulting from the high exothermic reaction nature, the reaction space velocities must be closely monitored (Fan et al., 2009). Therefore, as a result of the type of reactions (mainly endothermic), in all these reforming processes there is a need to introduce a catalyst that can increase the reaction rate and alter its pathway. Several researchers have tried to apply various catalysts to stimulate or change the reaction pathways and therefore either increase conversion or enhance longevity in conversion. In order to achieve this goal, several catalysts have been applied for different reforming process. For example, Nickel (Ni) catalyst have been used for steam reforming (Navarro et al., 2019), (Ali et al., 2016), CO_2 reforming (Li et al., 2018), (Li and Zhang, 2013), partial oxidation (Jalali et al., 2019), (Pelletier and Liu, 2007), auto-thermal reforming (Dega et al., 2019), bi-reforming (Siang et al., 2019) and tri-reforming (Zou et al., 2016), (Yoo et al., 2015). According to researchers, the functionality of these catalysts not only depends on the metallic active site, but also on the support and more specifically the promoters added to the catalyst formulation. Other researches have tried to find solution to deactivation of catalyst resulting from carbon deposited during the reforming of CH_4. Materials such as alumina (Lertwittayanon et al., 2017), (Kim et al., 2017), silica (Zhang et al., 2019), SBA-15 (Chong et al., 2019), (Abdullah et al., 2019), alkaline earth metals (Zhang et al., 2019), (Alipour et al., 2014), rare earth metals (lanthanide series)

(Jawad et al., 2019), (Al-Fatesh et al., 2014), have been used as catalysts/promoters or supports to solve the emanating issues of deactivation from carbon deposition. Amongst these supports, lanthanide series have been reported to have a huge impact on the removal of deposited carbon during CH_4 reforming processes. For examples, Ceria (CeO_2); one of the majorly used lanthanide series plays a key role in inhibiting the formation of carbon deposits by aiding its conversion. The compound CeO_2; contains Ce and a high amount of mobile O_2 vacancy sites formulated by replacing some of the Ce^{4+} ions present in the CeO_2 lattice with Ce^{3+} ions (Anjaneya et al., 2014). A lot of work has been done on the use of lanthanides series as catalyst/promoter or support in the reforming of CH_4. However, a detailed review on the role of lanthanide series on the various CH_4 reforming reactions such as; CO_2, partial oxidation, steam, tri and autothermal reforming need more attention. More also, comparison of the behavior of the lanthanide series in various CH_4 reforming reactions to ascertain the catalytic behavioral differences has not being widely reported to the best of our knowledge. Therefore, this study outlines the role played by the lanthanide series in various reforming processes for H_2 and syngas production. The specific properties of the lanthanide series that influences the reaction pathway of CH_4 reforming processes have been identified from reviews of existing literatures.

2. The role of lanthanide series in reforming processes

Researchers have used lanthanide series as promoter/catalyst and support in various reforming processes such as CO_2 (Khajeh Talkhoncheh and Haghighi, 2015), partial oxidation (Ferreira et al., 2010b), tri- reforming (Zou et al., 2016), autothermal (Escritori et al., 2009) and bi-reforming (Kumar et al., 2015). In addition, several hydrocarbons such as CH_4 (Omoregbe et al., 2016), ethanol (Da Silva et al., 2011), propane (Azizzadeh Fard et al., 2019), and glycerol (Bobadilla et al., 2015) can be reformed using these reforming processes/steps. In this section, we focus on various reforming processes for converting CH_4 to H_2 and CO, with specific interest on the influence of lanthanide series on the reaction pathway.

A commonly employed catalysts for CH_4 reforming process is Ni catalyst (Rathod and Bhale, 2014), (Jiang et al., 2007). Several researchers have employed Ni in CH_4 reforming reactions due to the industrial importance of Ni (Kim et al., 2015). Noble metals have also been extensively applied as catalyst in the reforming of CH_4 (Watanabe et al., 2016). However, in order for the reaction to shift in the forward direction, catalyst employed should be highly resistant to coking and possess high thermal stability (Singha et al., 2016). Hence, even though Ni is highly active for CH_4 reforming, the stability of Ni catalyst at elevated temperature cannot be guaranteed due to its high affinity towards coking which causes deactivation of the catalysts and termination of the reforming process. For this reason, recent studies on the reforming processes of CH_4 using metallic catalysts have been directed towards enhancing the morphology, reducibility and structure of the catalysts, so as to enhance catalyst performance (Anchieta et al., 2019). Consequently, according to Zhao et al. (2018), the inclusion of support with redox properties could reduce carbon deposition, eliminate sintering of the metal particles, increase the catalyst O_2 storage strength and enhance the behavioral interaction between the components of the catalysts. Several researchers have applied lanthanide series as catalyst (Zhu et al., 2018), promoter (Branco et al., 2020) and catalyst support (La Parola et al., 2018) to try to minimize/eradicate the problem of excessive carbon deposition. More also, with respect to their different structures and atomic sizes the members of this series can serve either as catalyst, promoter or support for different reaction processes. For instance, as catalyst, Zhu et al. (2018) applied $[Ln(CH_3CN)9]^{3+}[(AlCl_4)_3]^{3-}.CH_3CN$ (Ln = lanthanide series) as catalyst in the tandem Friedel-crafts alkylation reaction. When compared with $YbCl_3$, the increased activity of the catalyst was attributed to the Lewis acidic content of Yb species. In subsequent sub-sections of this paper, reviews on influence of the lanthanide series as catalyst/promoter and support in various reforming processes have been itemized from section 2.1 – 2.5.

2.1. Lanthanide series in CO_2 reforming of CH_4 (CRM).

2.1.1. Lanthanide series as catalyst/ promoter in CO_2 reforming of CH_4 (CRM)

One of the many reforming processes where CH_4 can be converted into H_2 and syngas is CRM. It is a catalytic reaction requiring the use of catalyst made up of several materials such as the transition metals and lanthanide series etc. Several authors have applied the lanthanides series as catalysts in this process. For instance, a structurally different type of support called the mesoporous carbon which was modified with lanthanides (Ce and La) was applied for CRM by Goscianska et al. (2018). The catalyst/support material was analyzed and the activity tested in CRM with result represented in Table 1. La and Ce catalysts on mesoporous carbons had better performance when compared with catalyst on SBA-15 and KIT-16. This was attributed to the introduction of La and Ce into the support material which resulted in an increment of the intensity of the peak observed in the XRD analysis. The peak represented changes in the support material, thereby reforming the hexagonal or cubic pore arrangement of the amorphous carbon (Goscianska et al., 2018), (Chen et al., 2013), (Maneerung et al., 2011). However, the textural analysis of the Ce and La based catalyst revealed reduced surface area when compared to the support's surface area. This led to reduction in pore size due to blockage as a result of the particles agglomerating during synthesis.

In another study by Gallego et al. (2009), $La_{1-x}A_xNiO_{3-\delta}$ perovskite catalyst (A = Pr, Ce and X = concentration of dopants) was prepared and utilized in CRM. The essence of their work was to ascertain the effects of Pr and Ce on the perovskite's performance. The catalyst $La_{0.9}Pr_{0.1}NiO_{3-\delta}$ had the optimum activity while possessing the ability to withstand about 100 h of reaction time with no deactivation observed. The considerable shift in the temperature of the hydrogenation patterns towards lower values which is described by the TPR profile represented in Fig. 1 is the reason for the improved activity. This catalytic property is also related to reduced NiO particle size also reported by Fan et al. (2009), coupled with the redox property of the Pr_2O_3 reported in similar work by Ayodele et al. (2017). Arguments were made that the Pr_2O_3 may become re-oxidized by CO_2 to form PrO_2 and CO in-situ reaction. As a follow up reaction, PrO_2 then combines with carbon deposits, thereby reforming Pr_2O_3 and gasifying the deposited carbon. The various arguments were linked to characterization of the catalyst material. For instance, the specific surface area of $La_{1-x}A_xNiO_{3-\delta}$ varied directly with the concentration of dopants, the XRD profile showed that increase in La and Ce varied directly with the formation of NiO and CeO_2. In addition, the concentration of dopants varied with the crystallite size of the perovskite. However, for the $La_{1-x}Pr_xNiO_{3-\delta}$ perovskite, no significant variance was observed in the crystallite size as the dopant concentration changed. This behavior was however not similar for a series of Ni-CeO_2 catalysts which declined in crystallite size when doped with La (Pino et al., 2011).

Another way the lanthanides series can be utilized in CRM is by applying it as promoter. In a study carried out by Habibi et al. (2014), La_2O_3 promoted Ni catalysts on γAl_2O_3 was synthesized and employed as catalysts in CRM. From the surface area analysis

Table 1
Activity parameters of CO_2 reforming of CH_4 (Goscianska et al., 2018).

Sample	Initial activity(mmolg^{-1}. min)	Activity after 1 h(mmolg^{-1}. min)	Catalyst deactivation [a] (%)	$K^c_{app\text{-}deac} \times 10^{-2}$ (min-1)	R^2 [d]
SBA-15	1.0	0.0	100[b]	–	–
5-La/SBA-15	4.6	0.6	87	3.79	0.967
5-Ce/SBA-15	5.0	2.4	52	1.08	0.832
$C_{SBA\text{-}15}$	0.5	0.0	100	–	–
5-La/$C_{SBA\text{-}15}$	5.4	1.0	81	2.83	0.977
5-Ce/$C_{SBA\text{-}15}$	7.1	3.8	46	0.97	0.987
KIT-6	1.0	0.0	100[b]	–	–
5-La/KIT-6	3.7	0.6	84	3.81	0.987
5-Ce/KIT-6	3.5	1.0	71	2.04	0.987
$C_{KIT\text{-}6}$	0.5	0.0	100	–	–
5-La/$C_{KIT\text{-}6}$	8.3	3.3	60	1.70	0.988
5-Ce/$C_{KIT\text{-}6}$	10.3	5.2	50	1.37	0.989

Reaction Conditions: 650 OC, 0.10 MPa, 1 h
c $K^c_{app\text{-}deac}$ from the linear regression: Ln(Initialactivity/activityattimet) = $k_{app-deac.}$ t.
d linear regression correlation factor
[a] Deactivation values after 1 h of reaction,(1 – activityafter1h/initialactivity)100
[b] Deactivation values after 30 min

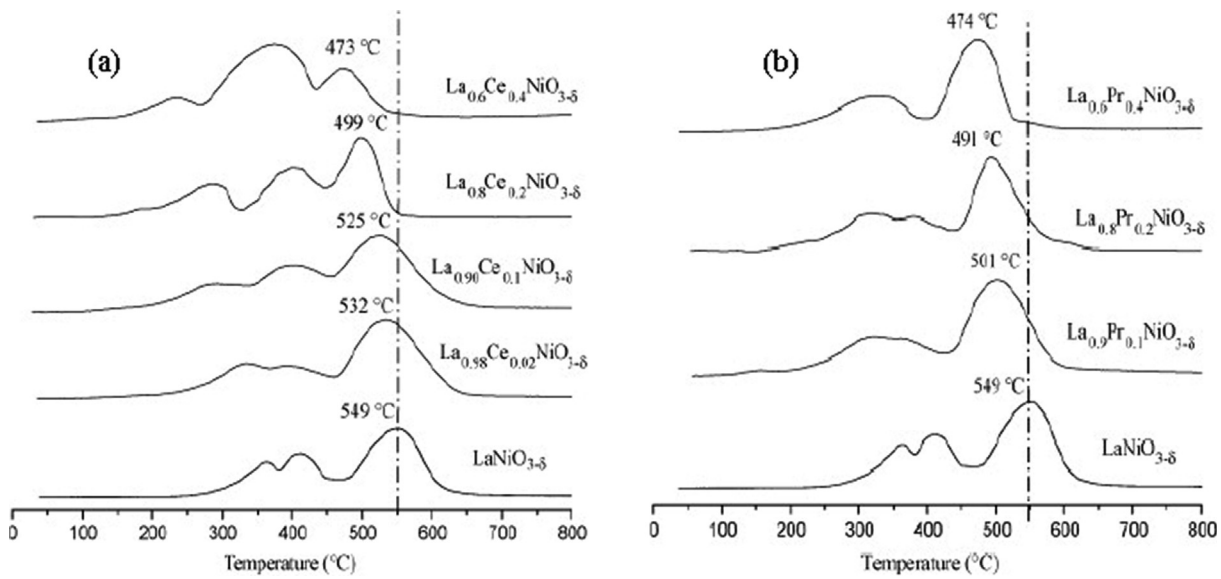

Fig. 1. TPR profile of (a) $La_{1-x}Ce_xNiO_{3-\delta}$ and (b) $La_{1-x}Pr_xNiO_{3-\delta}$ perovskites series (Gallego et al., 2009).

represented in Table 2, adding La_2O_3 to the Al_2O_3 reduced the specific surface area, a trend also reported for Ni on Al_2O_3 catalyst by Nandini et al. (2005), while TPR analysis revealed the addition of La_2O_3 aided the Ni reducibility, a phenomenon also reported by Rivas et al. (2008). Furthermore, the intensity of the reduced NiO peaks became higher with the addition of La_2O_3. This property affected the catalytic test carried out resulting in a substantial increase in the conversion of CH_4 with up to 3% La_2O_3 loading. Further studies carried out on the carbon deposits showed there was an inverse relationship between the addition La_2O_3 and the amount of carbon deposited up to 3 mol%.

Table 2
Textural properties of catalyst samples (Habibi et al., 2014).

Samples	BET (m^2g^{-1})	Volume (pore) (cm^3g^{-1})	Size (Pore) (nm)
Al_2O_3	204	0.41	5.30
1%La_2O_3-Al_2O_3	204	0.36	5.20
3%La_2O_3-Al_2O_3	196	0.34	4.90
6%La_2O_3-Al_2O_3	182	0.34	4.70
10%Ni/Al_2O_3	177	0.34	5.10
10%Ni/1% La_2O_3-Al_2O_3	183	0.32	4.90
10%Ni/3% La_2O_3-Al_2O_3	174	0.29	4.70
10%Ni/6% La_2O_3-Al_2O_3	169	0.28	4.60

[a]Obtained from the BET equation.
[b]BJH desorption pore volume.
[c] BJH desorption average pore diameter.

In a similar work, Charisiou et al. (2016) used CeO_2 and La_2O_3 to modify Ni/Al_2O_3 catalyst for CO_2 reforming of biogas. The performance of all the synthesized catalysts with respect to reaction temperature, reactants conversion and product yield were studied. They observed significant increase in the performance of the promoted Ni/Al_2O_3. The result of the stability test represented in Fig. 2 revealed Ni/Al_2O_3 catalyst (modified) remained active and stable for over 20 h, while the unmodified Ni/Al_2O_3 remained stable for only about 5 h. Also, according to De Llobet et al. (2013), Ni/Al_2O_3 catalyst produces syngas and filamentous carbon which does not deactivate the catalyst over 1 hr; a feat similar to the report by Charisiou et al. (2016).

In another work, Omoregbe et al. (2016) used La and Ce as promoters in a different type of support (SBA-15) for CRM. Upon

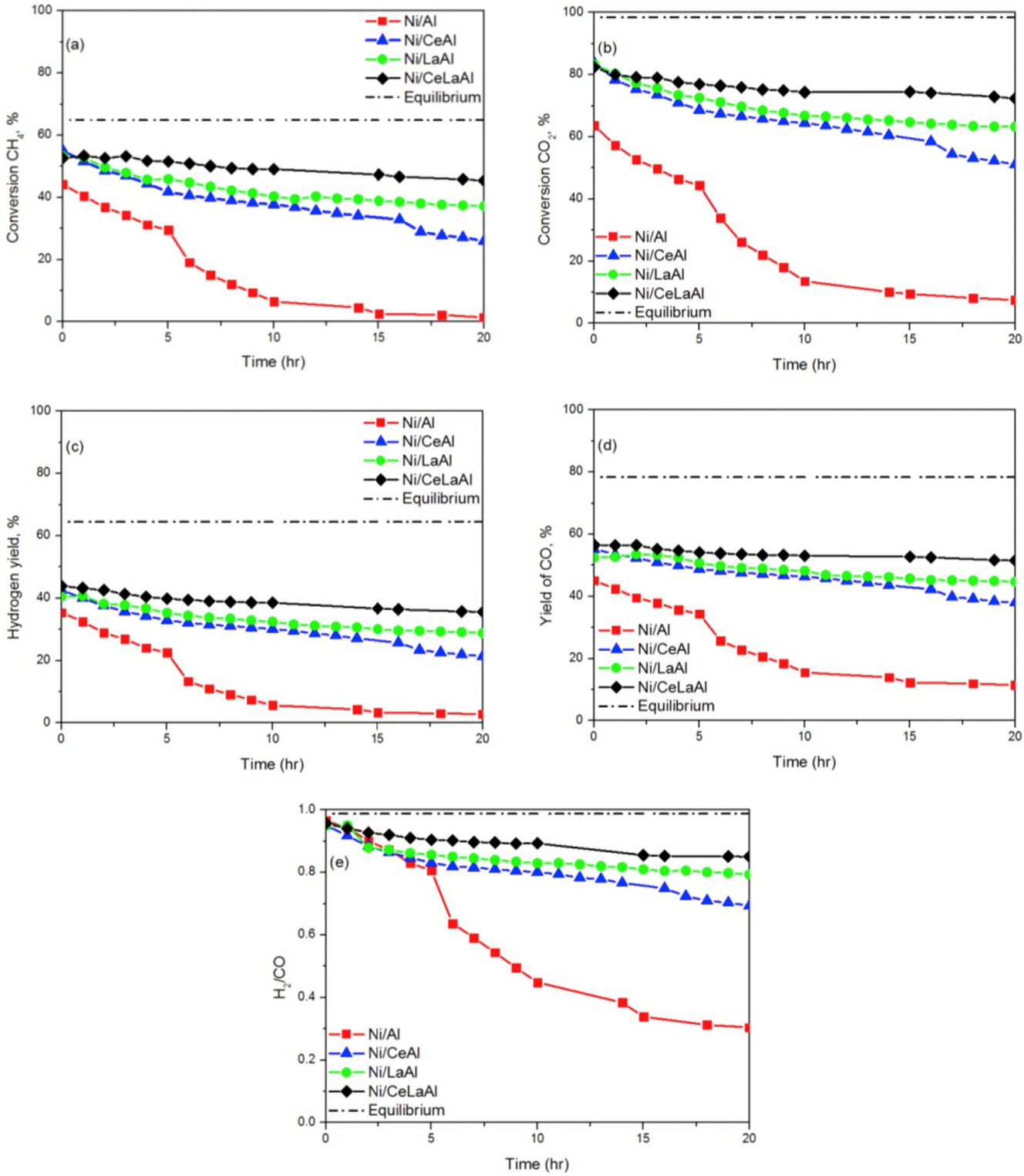

Fig. 2. Performance test for conversion and yield using Ni catalyst to modify CeO_2 and La_2O_3 on Al_2O_3 support (Charisiou et al., 2016).

promoting the catalyst, NiO reduced from 27.0 nm to 19.1 nm which could be traced to the interaction between NiO, La and Ce particles. TPO results were similar to the study by Akbari et al. (2018) where better performance associated with a decline in the deposited carbon was obtained for the 3 wt%-La promoted catalyst, while the un-promoted Ni/SBA-15 showed loss of activity over time. The catalyst with the smallest NiO particle size suppressed graphite carbon formation. Other authors' like Al-Fatesh et al. (2014) who used La_2O_3 as promoter and support for Ni/Al_2O_3 in CRM also stated that the incorporation of La_2O_3 into the catalyst structure enhanced the dispersion of Ni and subsequently the CO_2 adsorption which resulted in improved performance. Similarly, in the study by Sutthiumporn and Kawi, (2011) the performance enhancement of Ni-La_2O_3 catalyst was due to the

presence of abundance lattice O_2 which enhanced the C-H cracking in the reforming reaction. Also, Dębek et al. (2015), prepared NiMgAl mixed oxides and promoted it with Ce species before testing in CRM reaction. Post test results compared the performance with two reference catalyst 10Ni/Al_2O_3 and 10Ni/ (Ce-Zr). The introduction of Ce into the catalysts structure significantly improved the activity and selectivity. This is attributed to increased reducibility of Ni species resulting from introducing CeO_2 which contributes to enhance the basicity of the catalyst complex. In comparison with the reference catalyst; 10Ni/Al_2O_3 and 10Ni/(Ce-Zr), NiMgAl mixed oxides promoted with Ce showed better activity. The reference catalyst showed signs of deactivation and loss of activity in a 5 h time on stream (TOS) with CO_2 conversion lower in the 10Ni/(Ce-Zr) and excess CO produced in the 10Ni/Al_2O_3) catalyst. Akbari et al. (2018) also reported CeO_2 as promoter for CRM using Ni-MgO-Al_2O_3. Adding Ce to the catalyst Ni-MgO-Al_2O_3 influenced the size of the metallic crystals and the catalyst reducibility. In addition, carbon on the surface was greatly minimized; hence, conversion improved. Amongst all synthesized catalyst, the catalyst with 3 wt% Ce showed more resistance to coking. Furthermore, prior to addition of CeO_2, the reduction peaks from the TPR analysis located at maximum temperature depicted NiO reduction linked with the spinel phase (Wrobel et al., 1993). Whereas, for the Ni-MgO-Al_2O_3 doped with Ce, broad peaks which appeared at about 800 °C were linked to bulk CeO_2 reduction (Escritori et al., 2009). This is a significant shift in terms of the reduction capability of the Ce-Ni-MgO-Al_2O_3 catalyst. Hence, the catalyst behavior was viewed to be associated with the strong linkage between the metal and support resulting from a uniformly dispersed Ni on the support enhanced by doping with CeO_2 (Li et al., 2018), (Whang et al., 2017), (Abdullah et al., 2017). Fang et al. (2018) used a very similar catalyst for the same process and promoted with Ce and Nd. The textural analysis showed that the surface area was insufficient to ascertain the activity of the catalyst. The test carried out for the doped Ni/Mg-Al-O, pure Ni/Mg-Al-O, Ni/$MgAl_2O_4$ and Ni/Al_2O_3 catalyst revealed that the doped Ni/Mg-Al-O had better performance and appreciable reduction in the amount of carbon deposited. The catalytic behavior was ascribed to the improved Ni dispersion coupled with the availability of active surface O_2 as a result of addition of promoters (oxides of Ce and Nd) which aided reducibility according to the TPR results and similar studies (Harun et al., 2018), (Theofanidis et al., 2016). Furthermore, below 900 °C, there was no visible reduction of the Mg-Al-O support, which supports the claim that Al-O and Mg-O possess strong bond which are extremely difficult to reduce. At about 850 °C, the Ni/Al_2O_3 showed a main peak which depicted the reduction of $NiAl_2O_4$ (Abdollahifar et al., 2014). At 400 °C, the catalyst (doped and undoped) revealed a peak related to the reduction of Ni cations from NiO-MgO to Ni^o (Djaidja et al., 2006). Furthermore, catalyst stability was also enhanced when reduction occurred prior to the catalytic reaction step. The active surface area of Ni improved the catalyst's basicity resulting from the introduction/availability of active oxygen species supplied by the promoters.

Amin et al. (2015) used different lanthanide series (Nd, Ho, Eu, Er, Dy, Pr, Sm, Tm, Gd, and Tb) to alter the activity and structure of Ni/γ-Al_2O_3 in CRM. The promoted catalysts were far more superior to the unpromoted catalyst over a 60-h TOS. From all experiments they carried out, Er- Ni/γ-Al_2O_3 catalyst was seen to exhibit the optimum performance in terms of conversion of CH_4. They attributed the superior performance of Er- Ni/γ-Al_2O_3 to the optimum size of Ni particle and enhanced reducibility which led to reduced formation of reactive carbon during the reaction. However, some authors have also argued that increased Ni size may be as a result of carbon formed on the Ni particle. For instance, according to Han et al. (2017), Ni particle size increased due to catalyst deactivation resulting from carbon formation. Other authors who have studied lanthanide series as promoters and obtained similar results include; Foo et al. (2011) who used Ce, Pr and Sm to reduced carbon deposit by half and identified a reactive and unreactive type of carbon in CRM, Sarkar et al. (2016) who used Gd as promoter to obtain catalyst longevity of over 100 h TOS and Taherian et al. (2017) who reported at an optimum Sm wt% of 1, while obtaining a conversion of 58% at 700 °C with decreased rate of carbon formation.

2.1.2. Lanthanide series as support in CO_2 reforming of CH_4 (CRM)

Lanthanide series have been used in CRM as support for active catalysts. Usually, the catalysts are affixed to the support in order to create a larger surface area for the catalytic processes to occur. In a study carried out by Han et al. (2017), several Ni-Ce-Al oxides were prepared and applied for natural gas reforming of CO_2 to produce syngas. After several investigations, they selected 10 wt% Ni-CeAl catalyst and tested it in a 30 h reaction to ascertain its performance in CRM. Their results showed CH_4 and CO_2 conversion decreased by 2.8% and 2.6%, respectively. The result was achieved by the creation of the interlinking structure between NiO and CeO_2 formed by Ni^{2+} which bonded to the CeO_2 matrix replacing Ce^{4+} ions. Furthermore, as a result of charges imbalance and the disturbances created by the CeO_2 structure, O_2 vacancies were created in-situ reaction which aided gasification of the carbon deposits (Wang et al., 2013), (Shan et al., 2003). Li et al. (2017), used mesoporous silica enhanced with Nd as support for Ni catalyst in CRM. The process applied CO_2 and/or O_2 as the reformer to give syngas. Nd was embedded in the structure of mesoporous silica which in turn improved the metal (Ni) dispersion. The embedment which resulted in the dilation of the mesoporous silica peak was in conformity with the study by Chong et al. (2019). In addition, there was a direct relationship between the molar ratio of Nd/Si up to 0.04 and the point of inflection in the isotherm (P/P_o) which indicated an enlargement of the pore size (one of the importance of a good support) (Li and Zhang, 2013). Nonetheless, embedding Nd into the mesoporous structure reduced the catalyst BET surface area and pore volume but for the catalyst in the gas phase reaction, the pore size distribution which increased until 0.04 was more significant. In a similar analysis of textural properties, Li and Zhang (2013) also reported that surface area of Nickel/yttrium increased steadily as yttrium (Y) increased up to Y/Si = 0.04 and then decreased with continuous increase in yttrium content. For all molar ratio of the catalyst tested, Ni/0.04Nd-mesoporous silica gave the best performance in a 12 h TOS. The improved performance was linked to high dispersion of the Ni particle (Wang et al., 2012), increased basicity (Muñoz et al., 2013), coupled with the enhanced Ni-support inter-linkage (Li et al., 2017). Upon catalytic test over a longer time frame, the catalyst showed poor performance and high deactivation as a result of intensive oxidation of the Ni particle during reaction. Another way lanthanide series can be used for CRM is by modification of the support. Goula et al. (2017) tried this by modifying Zr using La_2O_3 and CeO_2-ZrO_2. Three supports; ZrO_2, La_2O_3-ZrO_2 and CeO_2-ZrO_2 were utilized on Ni for CRM. Surface areas of the catalysts obtained are represented in Table 3. Ni/Zr had the highest surface area value, followed by Ni/LaZr and Ni/CeZr. This behavior was ascribed to the difference in the pretreatment of the support during calcination (at 800 °C). Goula et al. (2015) also linked this kind of behavior to the blockage of the support pores by Ni ^{o} which occurs during calcination. Ni-LaZr and Ni-CeZr showed improved basicity and O_2 ion values as compared to Ni-Zr. This is reflected in the catalytic performance shown in Fig. 3 (a) – (e), where CH_4 conversion and H_2 production is much higher for catalyst containing lanthanide series than the plain Ni/Zr. Post reaction studies of the catalyst surface revealed filamentous tube-like carbon components of the graphitic 2H form present on the Ni/Zr and Ni/LaZr catalysts surfaces which Singha

Table 3
BET specific surface area (SSA) of the catalyst (calcined and reduced) (Goula et al., 2017).

Catalyst	Ni loading(wt%)	SSA(m^2 g^{-1})	Ni average particle size(nm)[a]	Ni dispersion (%)
Calcined Ni/Zr	7.7	50.0	15.7	4.2
Reduced Ni/Zr	7.7	43.0	23.0	2.9
Calcined Ni/LaZr	7.6	31.0	20.1	3.3
Reduced Ni/LaZr	7.6	29.0	20.2	3.3
Calcined Ni/CeZr	7.9	22.0	25.7	2.6
Reduced Ni/CeZr	7.9	28.0	15.2	4.3

[a] from Scherrer's equation.

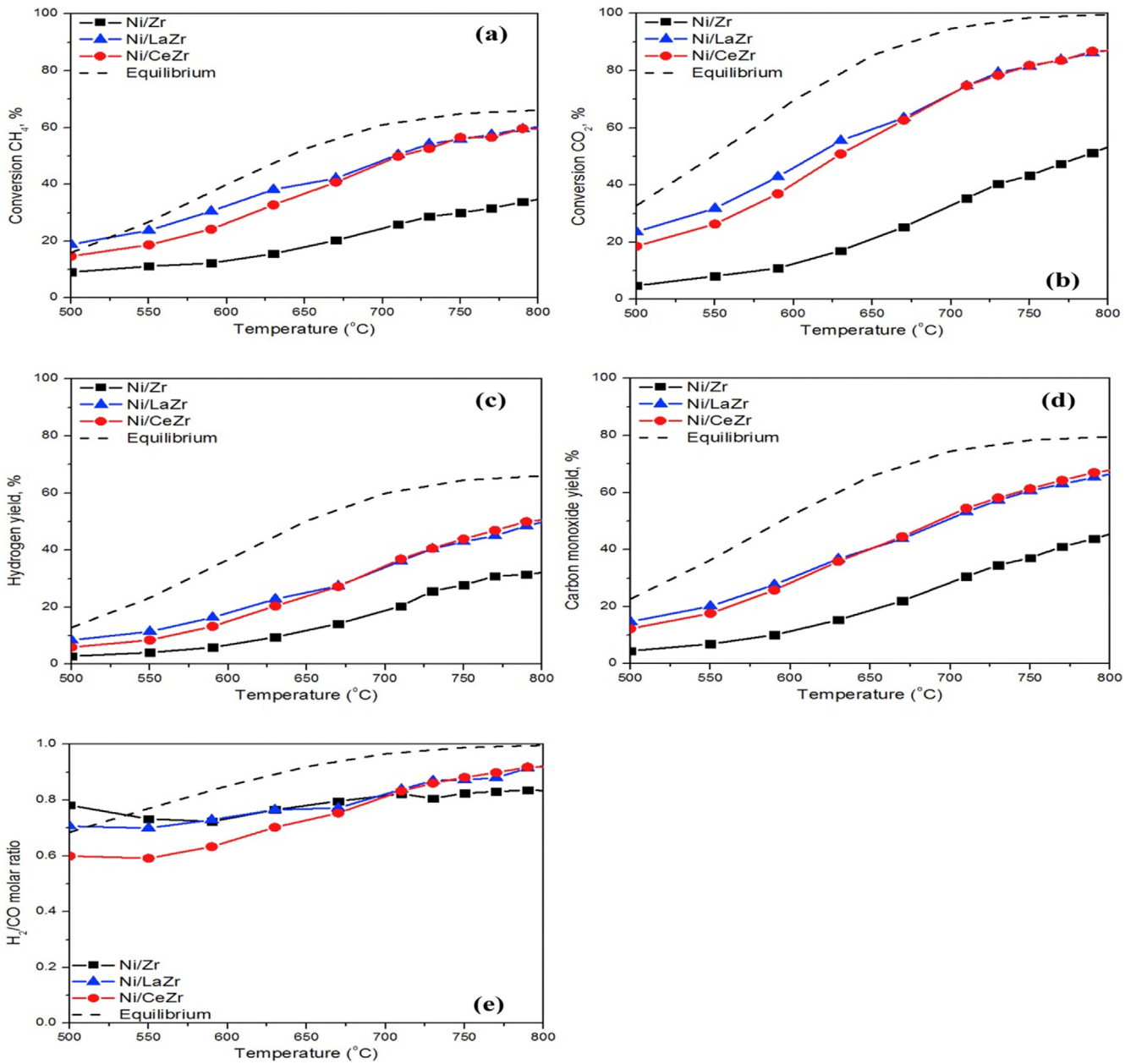

Fig. 3. Performance of Ni/Zr, Ni/CeZr and Ni/LaZr (Goula et al., 2017).

et al. (2017) also reported. Surprisingly, the Ni/CeZr spent catalyst had no traces of carbon deposits due to the high amount of lattice O_2 present in the Ni/CeZr catalyst. Ce has high O_2 storage capacity as a result of its ability to exist in various states of oxidation, thereby allowing it to take part in various redox processes using the carbon formed as its reactant (Otsuka et al., 1993). Also, according to Wang and Lu (1998), Nandini et al. (2005), and Laosiripojana et al. (2006), CeO_2 redox behavior coupled with its high availability of lattice O_2 are responsible for enhanced activity, stability as well as removal of carbon from the catalyst surface. Generally, embedding metals into the support matrix improves catalytic activity as revealed by Li et al. (2017) and De Rogatis

et al. (2010). In this sub-section, we have been able to identify some literature where lanthanide series have been applied as catalyst/promoter and support. Table 4 summarizes the literature reviewed in this section.

2.2. Lanthanide series in partial oxidation of CH_4 (POM).

2.2.1. Lanthanide series as the catalyst / promoter in partial oxidation of CH_4 (POM)

In this sub-section, the application of lanthanide series as catalyst/promoter in the partial oxidation of CH_4 has been reviewed. In a typical example, the partial oxidation of CH_4 using $LaNiO_2$, La_2NiO_4 in combination with CeO_2 was investigated by La Parola et al. (2018). At 60% conversion, the sample without CeO_2 deactivated rapidly, whereas the sample containing CeO_2 remained stable for 18 h TOS; same behavior reported by Nandini et al., (2005). In line with the mechanism, CH_4 cracking is activated by the presence of $LaNiO_3$-CeO_2 with the release of CO/CO_2 in a large temperature span thereby consuming the released carbon. Also, according to Feio et al. (2008) CH_4 conversion is highly dependent on the amount of CeO_2 added to the catalyst. The behavior was different for $LaNiO_3$ which cracks CH_4 in a narrow temperature span with no significant evolution of CO/CO_2 thereby allowing carbon to remain on the catalyst surface. This was further proven by the TPR analyses represented in Fig. 4 which portrayed good interaction between Ni and Ce resulting in better and improved performance (Wang and Lu, 1998). In addition, significant carbon was found in the catalyst without CeO_2, while the catalyst with CeO_2 had traces of carbon deposits.

Nd was also used in synthesizing $NdCaCoO_{3.96}$ for the partial oxidation of CH_4 by Dedov et al. (2015). In-situ reaction, $NdCaCoO_{3.96}$ decomposed to CaO, Nd_2O_3, Co and CoO resulting in 90% conversion of the reactants with over 90% selectivity of H_2/CO. The behavior of the catalyst over 140 h TOS was reported to be very stable. Even though formation of carbon was observed, this had no significant effect on the catalyst behavior. In another study, Ferreira et al. (2010b) prepared $CuCeO_2$ catalyst and tested the performance in the partial oxidation of CH_4 for 18 h. $CuCeO_2$ was stable at elevated reaction temperature; a property linked to the morphology of the catalyst. Post catalytic test results were CH_4 conversion of over 90%, H_2 selectivity of over 99% and syngas ratio of approximately 2.0 at 750 °C. CeO_2 and Cu interaction aided inhibition of the catalyst deactivation (Lima et al., 2006), (Tsipouriari and Verykios, 2001).

2.2.2. Lanthanide series as the support in partial oxidation of CH_4 (POM)

Applying lanthanide series as support for partial oxidation of CH_4, bimetallic Ni-lanthanide oxides (lanthanides = Pr, Gd and Lu) were prepared by Ferreira et al. (2010a). Result from the study suggests that the selectivity of the bi-metallic Ni-lanthanide oxides were derivatives from the conventional single metal oxide catalysts which are majorly reported in literature. When Gd or Lu was used to replace Pr, the catalyst activity was enhanced. The TPR profile related the shift to higher value of the temperature at maximum water evolution rate (Branco et al., 2008). Whereas, for the second reduction peak, the temperature at maximum water evolution rate for Pr is much higher (about 532 °C) than that of Gd. TPR analysis of Lu showed single reduction peak as against Pr which showed double peaks. Furthermore, there was a noticeable inter-linking effect between the two metallic oxides (NiO and Lu_2O_3). Hence, CH_4 conversions and product selectivity increased. Also, the performance of Gd and Lu metallic catalysts behaved similar to the conventional Pt catalyst (5 wt% Pt/Al_2O_3). In another study, where lanthanides series were applied as support, the effects of the interaction between the metal and support on the performance of Ni-CeO_2 during partial oxidation of CH_4 was reported by Singha et al. (2017). The highlight of this catalyst was its ability to resist deactivation during the partial oxidation of CH_4 while producing syngas of ratio approximately 2.0. Interestingly, the reduced temperature at which CH_4 was activated (400 °C) was largely as a result of the presence of CeO_2 as catalyst support (Laosiripojana et al., 2006). This finding is ascribed to the interactive effect between Ni ° and CeO_2 which aids gasification. Feio et al. (2008) also used lanthanide series as support; combining two types of supports; CeO_2 and Al_2O_3 to obtain the catalyst Pd/CeO_2-Al_2O_3 for partial oxidation of CH_4 studies. There is a direct relationship between CeO_2 loading and Pd crystalline size. This relationship is also affected by the increase in calcination temperature from 500 to 900 °C during preparation (Ruiz et al., 2008). This was evident in the surface area values obtained per weight of Al_2O_3. In contrast, the density of Pd sites varied inversely with CeO_2 loadings. This behavior was ascribed to the blockage of the metallic sites by lanthanide oxide species (Nandini et al., 2005). The control catalyst (Pd/Al_2O_3) had very poor longevity in the partial oxidation process as a result of excess carbon deposits, while as Ce loading increased, the catalysts became more resistant to coking, hence, better stability was observed. This is evident in the TPR analysis represented in Fig. 5 which shows increased consumption of H_2 for the catalyst promoted with CeO_2.

In this sub-section we have identified some literature where lanthanide series have been applied as catalyst/promoter and support for partial oxidation of CH_4. Table 5 represents a summary of selected literature reviewed in this paper.

2.3. Lanthanide series in steam reforming of CH_4 (SRM).

Lanthanide series have been employed in various steam reforming of CH_4 (SRM) studies (Kho et al., 2017), (Kyriakou et al., 2016), (Wattanathana et al., 2015). One of the elements of the series, CeO_2 (ceria), is particularly exceptional due to its high O_2 surface geometry which can be optimized to obtain a fully functional Hellmann–Feynman force storage capacity (OSC). This interesting property plays a key role in improving the resistance of metallic catalysts towards deactivation by carbon deposits, allowing rapid CH_x oxidation and CO or CO_2 release to the gas phase depending on experimental conditions (Purnomo et al., 2008), (Huang and Wang, 2007), (Xu et al., 2006). Interestingly, the lanthanide series can be employed as catalyst, promoter or support for SRM. Some existing works previously published are outline in this section.

2.3.1. Lanthanide series as the catalyst/promoter in steam reforming of CH_4 (SRM)

Lanthanide series can be applied as catalyst and promoter simultaneously. In a typical example of such study, un-promoted and promoted (Gd, Pr) CeO_2 catalysts were synthesized for steam reforming of CH_4 (SRM) by Florea et al. (2018). CeO_2 was used as catalyst due to its high O_2 storage capacity, mixed ionic electronic conductivity in a reducing environment and its good mechanical and thermal resistance. Pr enhanced the catalyst redox and catalytic properties by shifting the reduction temperature to a lower value, thereby indicating that substituting Ce^{4+} ions with other cations promotes anionic (O^{2-}) diffusion. Furthermore, Gd had a positive effect on the stability of the catalyst towards deactivation. This result was affirmed by Krishna et al. (2007) who also reported doping with lanthanide series such as Pr and Gd minimized or eradicated CeO_2 sintering during reforming processes. Lanthanide series can also be applied as promoter and catalyst for SRM. For instance, Salcedo et al. (2018) synthesized Pr-promoted CeO_2 based catalyst for CH_4 activation in steam reforming process. Firstly, the use of CeO_2 as support ensured availability of lattice

Table 4
Lanthanide series in CO_2 reforming of CH_4 (CRM).

Reforming processes	Catalyst type	Lanthanide series	Function of lanthanide series	Aim of study	Outcome of study	References
CRM	La and Ce- carbon/ SBA-15 and/or KIT-6	La and Ce	Catalyst	Investigation of the catalyst performance	• Better performance when compared to SBA-15 and KIT-6 • Decreased surface area on the introduction of La and Ce	(Goscianska et al., 2018)
	$La_{1-x}A_xNiO_{3-\delta}$	Ce and Pr	Catalyst	Effects of Ce and Pr on performance	• CH_4 and CO_2 conversion of 49% and 55%, syngas ratio 0.81 • Longevity up to 100 h of reaction time • No deactivation observed	(Gallego et al., 2009)
	Ni-γAL_2O_3	La_2O_3	Promoter	Improve Catalystperformance	• Reduced surface area • Increased NI reducibility • Optimum La_2O_3 loading was 3 wt%. • Inverse relationship between amount of carbon deposited and La_2O_3 loading up to 3 wt%	(Habibi et al., 2014)
	Ni/Al_2O_3	CeO_2 and La_2O_3	Promoter	Catalyst performance	• La_2O_3 promoted catalyst had optimum performance	(Charisiou et al., 2016)
	Ni-SBA-15	La and Ce	Promoter	Synthesis and catalytic testing	• Addition of promoter reduced the NiO oxide phase from 27 nm to 19.1 nm • Using 3%- La-10%-Ni-SBA_{15} reduced the amount of carbon deposit • 3% La-10%Ni/SBA-15 suppressed the formation of graphite carbon	(Omoregbe et al., 2016)
	Ni/-Al_2O_3	La_2O_3	promoter and support	Synthesis and catalytic test	• Enhanced dispersion of Ni and CO_2 adsorption	(Al-Fatesh et al., 2014)
	NiMgAl mixed oxides	Ce	Promoter	Effect of Ce on performance	• Improved performance • Basicity enhanced	(Dębek et al., 2015)
	Ni-MgO-Al_2O_3	CeO_2	Promoter	Improve catalyst performance	• Alters the size of Ni crystals • Improved reducibility • Minimized carbon deposits • Improved conversion of reactants • 3 wt% of Ce loading had highest coking resistance	(Akbari et al., 2018)
	Ni/MgO-Al-O	Ce and Nd oxides	Promoter	Catalytic test and characterization	• Surface area was insignificant in relation to catalyst performance • Promoted Ni/MgO-Al-O showed better performance • Reduced carbon deposit • Reduction prior to catalyst test improve the stability of the catalyst	(Fang et al., 2018)
	Ni-γAL_2O_3	Tb, Tm Pr, Sm, Gd, Nd, , Er, Dy, Eu, Ho,	Promoter	Alter the structure and performance	• Initial low conversion due to reduced pore sizes. • Longevity up to 60 h showed improved performance of promoted catalysts • Reduced carbon deposits • Er- Ni/γ-Al_2O_3 exhibited the optimum performance	(Amin et al., 2015)
	Co-Ni catalysts on alumina	Ce, Pr and Sm	Promoter	Effect of Ce, Pr and Sm as promoter on performance	• Ce, Pr and Sm had no effect on consumption rate of reactants • Increase in production rate • Carbon deposit reduced by half • Resistance to carbon; Ce > Pr > Sm • Two types of carbon were observed (reactive and unreactive)	(Foo et al., 2011b)
	GdNi/ZSM-5	Gd	Promoter	Effect of mass transfer	• Increased mass transfer of the reactants • Increased O_2 mobility • Longevity over 100 h of reaction	(Sarkar et al., 2016)
	Ni and Co/SBA/15	Sm	Promoter	Tested in CRM	• Optimum Sm wt % was 1 wt%. • Sm-Ni/SBA-15 had the best conversion of 58% at 700 °C • Decrease rate of carbon formation	(Taherian et al., 2017)
	Ni-Ce-Al oxides	Ce-Al	Support	Synthesis and catalytic test	• CH_4 and CO_2 conversion reduced with a 2.8% and 2.6%, respectively after 30 h using Ni/10-Ce-Al • Improved gasification of carbon deposit	(Han et al., 2017)
	Ni catalyst	Mesoporous silica enhanced with Nd	support	Synthesis and catalytic test	• Improved metal dispersion • Direct relationship between the molar ratio of the support; Nd/Si and pore size enlargement • Reduction in the area and volume of the pores.	(B. Li et al., 2017)

(*continued on next page*)

Table 4 (*continued*)

Reforming processes	Catalyst type	Lanthanide series	Function of lanthanide series	Aim of study	Outcome of study	References
	Ni-Zr	CeO_2 and La_2O_3	Support	Syngas from biogas CO_2 reforming	• For gas phase reactions, pore size distribution is more significant • Ni/0.04Nd/Si gave the best performance for a 12 h reaction run • Poor stability and high deactivation • Incorporation of La and Ce reduced surface area in the order Ni/LaZr > Ni/CeZr. • Ni/LaZr and Ni/CeZr showed improved basicity when compared to Ni-Zr • Improved catalytic performance • Filamentous tube-like carbon deposited on Ni-Zr and Ni/LaZr • Ni/CeZr spent catalyst had no carbon tube-like deposits.	(Goula et al., 2017)

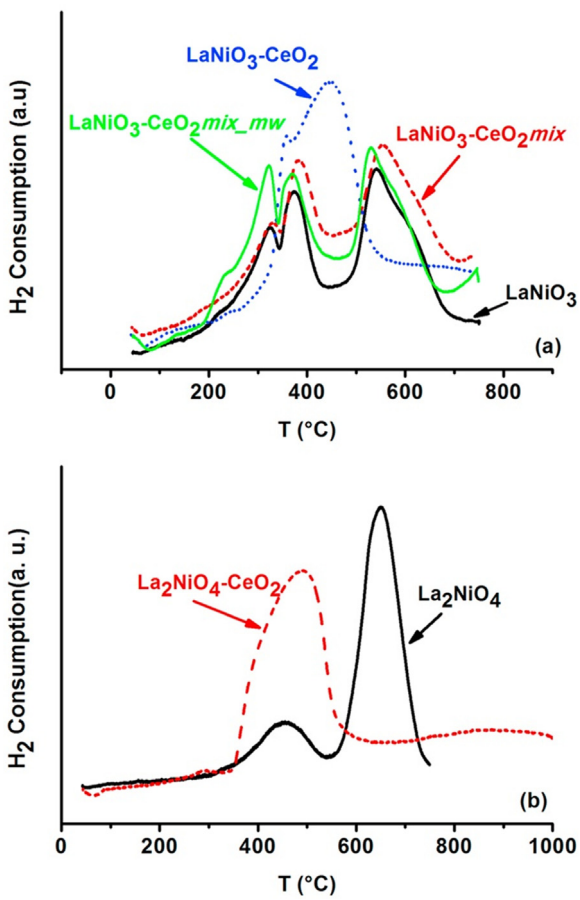

Fig. 4. TPR profile of the various Ni-based catalysts (a) perovskite formulation (b) spinel containing samples (La Parola et al., 2018).

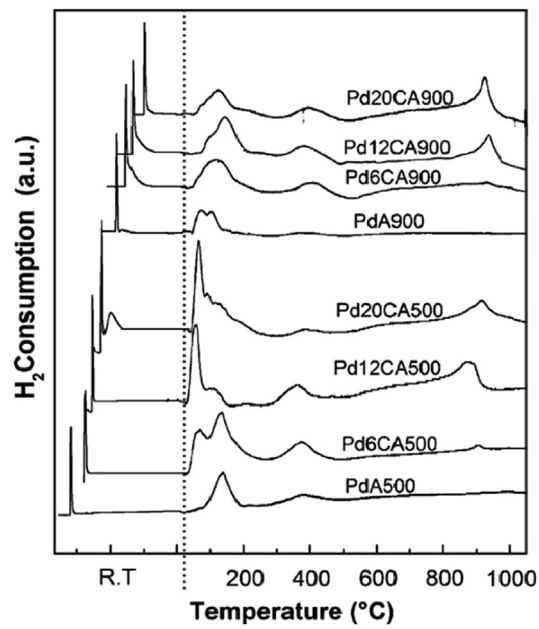

Fig. 5. TPR profile of Pd/Al_2O_3 (PDA) and $Pd/xCeO_2$-Al_2O_3 catalysts from supports calcined at 500 °C and 900 °C (xCA900) with varying load CeO_2 wt. % (Feio et al., 2008).

O_2. Subsequent doping of the catalyst with Pr improved the O_2 storage capacity of the catalyst. The closeness of the ionic radii of Pr (0.97 Å) and Ce (0.96 Å) was responsible for the increased O_2 storage capacity (Shannon, 1976). Hence, movement of O_2 species was enhanced without any significant change in the crystal structure (Gupta et al., 2010), (Chiba et al., 2009). In addition, the Pr-promoted CeO_2 catalyst surface had lower energy requirement for the formation of O_2 vacancy than the pure CeO_2 (Milberg et al., 2017), (Poggio-Fraccari et al., 2014), (Poggio-Fraccari et al., 2013). The ability of Pr to form Pr^{4+}/Pr^{3+} reduction–oxidation pair allows for improved reduction capability of Ni CeO_2-based catalyst hence, enhancing the catalyst ability to oxidize carbon at the catalyst surface. In a similar study, Harshini et al. (2014) synthesized un-promoted and promoted (Pr) Ni/CeO_2-hafnia based metal oxides and tested the effect of the support and promoter in SRM. The Ni/CeO_2-hafnia-Pr promoted catalyst had better performance over Ni/ CeO_2-hafnia un-promoted catalyst as a result of the enhanced O_2 mobility of the promoted catalyst. Also, the redox ability and size of the promoter played a major role in enhancing the O_2 storage capacity (OSC) of the CeO_2 supported catalyst.

In an attempt to control the selectivity of SRM, La and Ce was employed as promoters for Ni/Al_2O_3-MO (M: La, Ce) by Gubareni et al. (2018). The highest selectivity for CO was obtained with the Ni/Al_2O_3-CeO_2/cordierite catalyst. The decrease in the rate of the water gas shift reaction was the main reason for the result obtained with the Ce containing catalyst. In addition, the amount of CO_2 by-products decreased significantly in the presence of Ni-CeO_2-Al_2O_3/-cordierite catalyst due to O_2 from the CeO_2 structure oxidizing the carbon deposited on the active sites. Also, the presence of CeO_2 in the catalyst slightly reduced the Lewis acid sites, while La_2O_3 yielded two types of Lewis acid sites; La^{3+} cation responsible for the dissociative adsorption of water vapor and

Table 5
Lanthanide series in partial oxidation of CH_4 (POM).

Reforming processes	Catalyst type	Lanthanide series	Function of lanthanide series	Aim of study	Outcome of study	References
POM	$LaNiO_2$ and La_2NiO_4	La and Ce	Catalyst and Promoter	Catalytic test and CH_4 reforming	• Sample without CeO_2 deactivated after reaching 60% • Sample with CeO_2 remained stable for 18 h TOS • $LaNiO_3$-CeO_2 activated CH_4 decomposition in a wide temperature span • $LaNiO_3$ activated CH_4 decomposition in a narrow temperature span. • $LaNiO_3$ had carbon deposits while $LaNiO_3$-CeO_2 had traces of carbon deposits	(La Parola et al., 2018)
	$NdCaCoO_{3.96}$	Nd	Catalyst	Production of syngas	• 90% conversion of CH_4 O_2 • 90% selectivity of H_2/CO • Catalyst stable over 140 h TOS. • Carbon was formed but no significant effect on the activity.	(Dedov et al., 2015)
	$CuCeO_2$	Ce	catalyst	Catalytic test and CH_4 reforming	• CeO_2 and Cu interaction inhibited catalyst deactivation • Catalyst stable over high tempertaure	(Ferreira et al., 2010b)
	Ni-lanthanide oxides	Pr, Gd and Lu	Support	Synthesized and applied as catalyst	• Gd and Lu enhances catalytic activity more than Pr • Lu showed single reduction peaks as against Pr with double reduction peaks • Gd and Lu performance was similar to 5 wt% Pt/Al_2O_3.	(Ferreira et al., 2010a)
	Ni catalyst	CeO_2	Support	Performance of catalyst	• High ability to resist carbon formation • Syngas ratio of about 2. • Reduced CH_4 activation temperature (400 °C)	(Singha et al., 2017)
	Pd/CeO_2-Al_2O_3	CeO_2	Support	Catalyst synthesis and activity	• Direct relationship between CeO_2 loading and Ce crystalline size. • The density of Pt sites varied inversely with CeO_2 loading • CeO_2 loading improved the catalytic stability	(Feio et al., 2008).

the Al^{3+} cation (Del Angel et al., 2005). Hence, CeO_2 did not function as a Lewis acid site.

Employing a different type of support, Arcotumapathy et al. (2015) promoted Ni/SBA-15 with Ce and tested the catalyst in SRM. Promoting with Ce decreased the acid-to-base concentration of the catalyst by about 12%. Srivastava et al. (2006) had previously reported that SBA-15 possesses weak Lewis acid and basic sites at between 465 and 690 K and 365–430 K, respectively. Alumina support on Ce promoter was also used by Duarte et al. (2014) to carry out transient pulse studies to ascertain the catalytic effects of the catalyst on the reaction steps in SRM. CeO_2 catalyzed the oxidation of carbon. Several other authors have attempted to establish the relevance of the support to the kinetic step in SRM. For instance, Halabi et al. (2010a) and Halabi et al. (2010b) reported a mechanism where the activation of CH_4 occurred on rhodium while H_2O was adsorbed on CeO_2. According to Craciun et al. (2002), metal-support interaction is vital for the catalyst activity, Kurungot and Yamaguchi (2004) revealed that the results obtained from Rh/Al_2O_3 catalysts was due to the O_2 storage capacity of CeO_2 which aided minimization of carbon deposition during the SRM process. Furthermore, according to Zhuang et al. (1991), CeO_2 enhanced the CH_x species and H_2O reaction at the metal and support interface. Hence, it significantly suppressed the formation of carbon deposits, thereby allowing the catalyst to remain active. Moreover, the rate at which CH_4 was activated increased with the degree of metal support interaction and dispersion (Van Santen, 2009). Other authors like Berger-Karin et al. (2012), Buyevskaya et al. (1994) claimed CH_4 cracking to carbon occurred on the reduced metallic sites. Hence, the overall rate of reaction depends on surface O_2 availability and type of support.

2.3.2. Lanthanide series as support in steam reforming of CH_4 (SRM).

Iglesias et al. (2019b) prepared Zr promoted Ni catalyst supported on CeO_2 for steam reforming of CH_4 (SRM) varying the feed ratios and contact time. The main role of CeO_2 was to improve the chances of gasification during the reaction process. During the reaction, as more carbon is produced, the chances of producing CO_2 reduce. However, with the presence of CeO_2 which has a high lattice O_2 storage, conversion of carbon to CO_2 was achieved and enhanced. In similar studies by Ochoa et al. (2017) and Zhang and Verykios (1994), as time of stream increased, the chances of gasification occurring reduced due to the presence of excess carbon. In another work by Iglesias et al. (2019a), Ni catalyst on Zr and CeO_2 support was prepared and characterized in order to obtain a deeper understanding of the interaction between the catalyst and CeO_2 support. Even though addition of Zr significantly enhanced the O_2 mobility (Aneggi et al., 2006), (Bedrane et al., 2002), (Boaro et al., 2000), the O_2 storage capacity was higher for catalyst with $CeO_{2-\delta}$ support (104 μmol CO_2 g^{-1}) than for the catalyst doped with Zr (less than100 μmol CO_2 g^{-1}). This had a significant effect on the catalyst reduction as Ni and CeO_2 reduced effectively in the low temperature region, hence, confirming good Ni/ CeO_2 support interaction. In another study, Iglesias et al. (2017) synthesized Ni based catalysts on pure and promoted CeO_2 (5% Zr, Pr, and La) for SRM under mild conditions. High reducibility which led to better catalytic activity was observed for catalysts calcined at 750 °C as a result of Ni-Ce interaction. Furthermore, promoting CeO_2 with other lanthanide series ensured the combination of CeO_2 with trivalent cations like La^{3+} and Pr^{3+} to produce vacancies which created electronegativity in the catalyst. Moreover, these vacancies favored O_2 mobility within the CeO_2 structure. Previous studies by Poggio-Fraccari et al. (2014) and Ran et al. (2011) reported similar increase in O_2 mobility when Pr was employed as a promoter. Cheah et al. (2018) studied SRM over Ir/$Ce_{0.9}Gd_{0.1}O_{2-x}$ (Ir/CGO) catalyst. The activity of this catalyst was totally dependent on the metallic site (Ir site). This site was responsible for the activity while the support (CGO) influenced the reduction of carbon on the catalyst surface. During the reaction

process, Ir was completely reduced, thereby resulting in smaller particle size of 1.7 nm. The complete reduction was attributed to the very good synergistic interaction between the metal and the support during the reaction. After complete reduction, the activity improved as a result of synergistic interaction between well dispersed metal species interacting with CGO support during the reaction process. According to Mosqueda et al. (2009), CGO catalyst activated CH_4 forming reactive CH_x species, thereby reducing Ce^{4+} to Ce^{3+} and producing syngas. Therefore, the steam reforming reaction rate is dependent on the slow reaction of CH_4 with O_2 present in the promoted- CeO_2 and the fast reaction between water and already reduced CGO (Ramírez-Cabrera et al., 2004). Postole et al. (2015) provided an efficient iridium-doped CeO_2 catalyst prepared by solution combustion for SRM. The effect of support on the catalyst was tested and compared to result obtained from the same catalyst prepared by wet impregnation method. Furthermore, the activity of Ir-CeO_2, Ir/SiO_2-Al_2O_3 and Rh-CeO_2 were compared in the SRM process. The use of CeO_2 as support and Ir as catalyst ensured the process was highly efficient for SRM in terms of carbon resistant and permanent removal of sulfur poisoning. Ir/Si-Al_2O_3 deactivated in the presence of sulfur, while Rh-CeO_2 was unable to obtain initial activity after being exposed to feed containing H_2S. The performance of SRM lies in the in-situ reaction balance between CH_4 decomposition rate over the metal particles and the carbon removal rate from the catalyst surface. Hence, as a result of its excellent reduction–oxidation properties, CeO_2 strives in this kind of process which entails oxidizing the carbonaceous deposits on the catalyst surface during reaction (Höhlein et al., 2000). A comparison of CeO_2 and Al_2O_3 supported catalyst was carried out by Italiano et al. (2018). Rh catalysts supported on CeO_2, CeO_2-Al_2O_3 and Al_2O_3 for SRM were prepared. The results were in line with conclusion reached by Goula et al. (2017), Vita et al. (2014), and Bereketidou and Goula, (2012), where lanthanide series metals like CeO_2 were responsible for inhibiting carbon formation due to their excellent redox properties and capacity to store O_2.

In this sub-section, literatures where lanthanide series have been employed as catalyst/promoter and support for steam reforming of CH_4 have been reviewed. Table 6 represents a summary of selected literature reviewed.

2.4. Lanthanide series in Tri-reforming of CH_4 (TRM).

2.4.1. Lanthanide series as catalyst / promoter in tri-reforming of CH_4 (TRM

The main aims of combining various reforming processes is to tilt the reaction towards a particular product and to effectively control the deposition of carbonaceous compounds which deactivates the catalyst in methane reactions. In order to obtain these goals, researchers have used processes like bi-reforming (Siang et al., 2019), (Singh et al., 2018) and tri-reforming (Alipour-Dehkordi and Khademi, 2020), (Fedorova et al., 2020) of methane reaction. These processes allow for more effective catalyst usage as there would be less carbon available to deactivate the catalyst. Adding water (bi reforming) and O_2 (tri-reforming) to the reactants oxidizes the carbon species (Kumar et al., 2015). In this sub-section we focus on the role of lanthanide series in the tri-reforming of methane as it offers better route for gasification of carbon due to the added advantage of more oxidants such as CO_2, H_2O and O_2 in one process. Moreover, the addition of steam and O_2 enhances the efficiency of the methane reforming process (Fedorova et al., 2020). Studies on the application of lanthanide series as catalyst/promoter in the TRM have been discussed in this section. In one of such studies, simultaneous CO_2, steam and partial O_2 reforming of CH_4 known as tri-reforming of CH_4 was reported by Pino et al. (2011). La- doped Ni-CeO_2 were synthesized and used for TRM. Promoting the Ni-CeO_2 catalyst with La (10 at %) improved the reactants conversion from 93% and 83% to 96% and 86.5%, respectively. However, promoting Ni-CeO_2 with La of more than 10 wt% as shown in Fig. 6 resulted in a drop in conversion of reactants and product ratio, respectively. The increment was ascribed to the surface O_2 vacancies of Ce present in the active sites (Su et al., 2014), (Shyu et al., 1988). This effect aids Ni-dispersion by improving the basicity of the catalyst, hence, creating improved interaction of surfaces with CO_2 (Anchieta et al., 2019).

In a recent study, Zr, Ce and Ce-Zr were applied as promoters on Ni/$MgAl_2O_4$ and tested in TRM by Lino et al. (2019). Two reaction temperatures were tested; 650 °C and 750 °C. Deposits of carbon which were attached to the catalyst surface during reaction were minimized in the catalyst promoted by Zr and Ce-Zr, and this led to improved conversion of reactants. Furthermore, filamentous carbon formed during reaction using the un-promoted catalyst is responsible for the instability in the catalyst; an idea shared by other researchers who carried out similar studies (Lino et al., 2019) ,(Kambolis et al., 2010), (Ermakova et al., 2001). The drift to lower Ni $2p^{3/2}$ binding energy in the fresh Ni-Ce-Zi-Mg-Al catalyst spectra when compared with the spectra of fresh Ni-Mg-Al catalyst was responsible for this behavior. In the course of this shift, electron is transferred from the promoters Zr and Ce to the Ni. Hence, Lino et al. (2019) related the transfer of electrons to the consumption of H_2 tabulated in Table 7. Furthermore, the electron transfer is as a result of the chemical reaction resulting from the incorporation of Zr and Ce into NiO. For the Ni-Ce-Mg-Al catalyst, there was a shift to a lower binding energy as a result of the electron transfer which occurred between Ni and Ce (Daza et al., 2011). In addition, for the Ni-Ce-Mg-Al catalyst, the uniform dispersion rather than the interaction between Ni and Ce was responsible for the strong metal support interaction (Kaddeche et al., 2017). Thus, the amount of carbon deposited was in the order: NMA > NCZMA > NZMA ~ NCMA. Hence, the promoters aided the modification of the basic site component of the catalysts, thereby reducing the filamentous carbon type which remained as carbon deposits on the Ni-Mg-Al catalyst during reaction.

In their quest to improve H_2 production, Izquierdo et al. (2013) used catalysts with varying Ni and Rh-Ni on Mg or Al_2O_3 support promoted with CeO_2 and ZrO_2. Rh-Ni/Ce-Al_2O_3 produced the maximum amount of H_2 for O_2/CH_4 = 0.25 and S/C ratio of 1.0 in CRM and TRM. The catalyst behavior was attributed to the metal particles which were uniformly dispersed. Using similar operating conditions, Ni-Ce-Zr-Al_2O_3 had the highest production of H_2 for biogas tri-reforming. Furthermore, emphasizing on the structural buildup of the catalyst for TRM, varying sizes of York-Ni-Ce-@SiO_2 multi-York shell nanotube represented in Fig. 7 was synthesized and applied in TRM (Kim et al., 2019). The conventional Ni-Ce-/SiO_2 synthesized by impregnation technique showed lesser stability than the Ni-Ce-@SiO_2 multi-York shell nanotube catalyst material. This behavior is ascribed to the morphological and synergistic linkages between Ni/Ce and Ni/Si species. When using 1.0 reactant ratio, Ni-Ce-@-SiO_2 catalyst with yolk less than 20 nm showed better carbon resistance than NiCe@SiO_2 of larger sized yolks. This could be related to oxidation of carbon as explained by Wang et al. (2003). Whereas, NiCe@SiO_2 with larger sizes (i.e. yolk size greater than 30 nm) showed better stability in TRM at increased reactant ratio of 1.10. The deactivation of Ni-Ce-@-SiO_2 when smaller York sizes at 1.1 reactant ratio was used is attributable to the re-oxidation of Ni active species controlled by the redox characteristics of Ce^{3+}/Ce^{4+}, formation of carbon and the oxidation rates. As further proof, Table 8 shows that the ratio of α/β H_2 uptake for Ni-Ce-@-SiO_2 multi-York-shell nanotube (^{A} and ^{C} = water to surfactant ratio) was much larger than that of the Ni-Ce/SiO_2 impregnation

Table 6
Lanthanide series in steam reforming of CH_4 (SRM).

Reforming processes	Catalyst type	Lanthanide series	Function of lanthanide series	Aim of study	Outcome of study	References
SRM	Pr-Ce catalyst	Pr and Ce	Catalyst/ Promoter	Investigation of the catalyst performance	• Availability of lattice O_2 due to presence of Ce • Increased O_2 storage capacity	(Salcedo et al., 2018)
	Ni/ceria-hafnia	Pr and Ce	Promoter/ support	To improve performance	• Enhanced O_2 mobility	(Harshini et al., 2014)
	Ce- (Gd, Pr) catalyst	Ce, Gd, Pr	Catalyst/ Promoter	Investigation of catalyst performance	• Reduction temperature was shifted to lower values • Enhanced redox and catalytic properties	(Florea et al., 2018)
	Ni/Al_2O_3-M_xO_y	La. Ce	Promoter	Controlling the selectivity of SRM	• Ni/Al_2O_3-CeO_2 had the highest selectivity • Decreased CO_2 by-products • La_2O_3 yields two types of Lewis acid sites	(Gubareni et al., 2018)
	Ce-Ni/SBA-15	Ce	Promoter	Activity test for SRM	• Decreased acid-base concentration of the catalyst by 12%	(Arcotumapathy et al., 2015)
	Ce-Al_2O_3	Ce	Promoter	Catalytic effect of catalyst in SRM	• Effective oxidation of carbon	(Duarte et al., 2014)
	Zr-Ni/Ceria	Ce	Support	Investigation of the catalyst performance	• Enhanced gasification • Increased CO_2 production	(Iglesias et al., 2019b)
	Zr-Ni/Ceria	Ce	Support	Preparation and characterization	• High O_2 storage capacity	(Iglesias et al., 2019a)
	Ni/Ce- (5%, Zr, Pr and La)	Ce, La and Pr	Promoter/ Support	Investigation of the catalyst performance	• High reducibility • High catalytic activity • Good Ni-Ce interaction • Improved O_2 mobility	(Iglesias et al., 2017)
	$Ir/Ce_{0.9}Gd_{0.1}O_{2-x}$	Ce, Gd	Support	Investigating steam reforming of CH_4	• Reduction of carbon on catalyst surface • Good synergistic interaction between Ir and support	(Cheah et al., 2018)
	Ir/CeO_2		Support	Activity test for SRM	• High carbon resistant • Permanent removal of sulfur poisoning	(Postole et al., 2015)
	Rh catalysts supported on CeO_2, CeO_2-Al_2O_3 and Al_2O_3	Ce	Support	Activity test for SRM	• Inhibition of carbon • Improved redox properties • Availability of O_2 storage capacity	(Italiano et al., 2018)

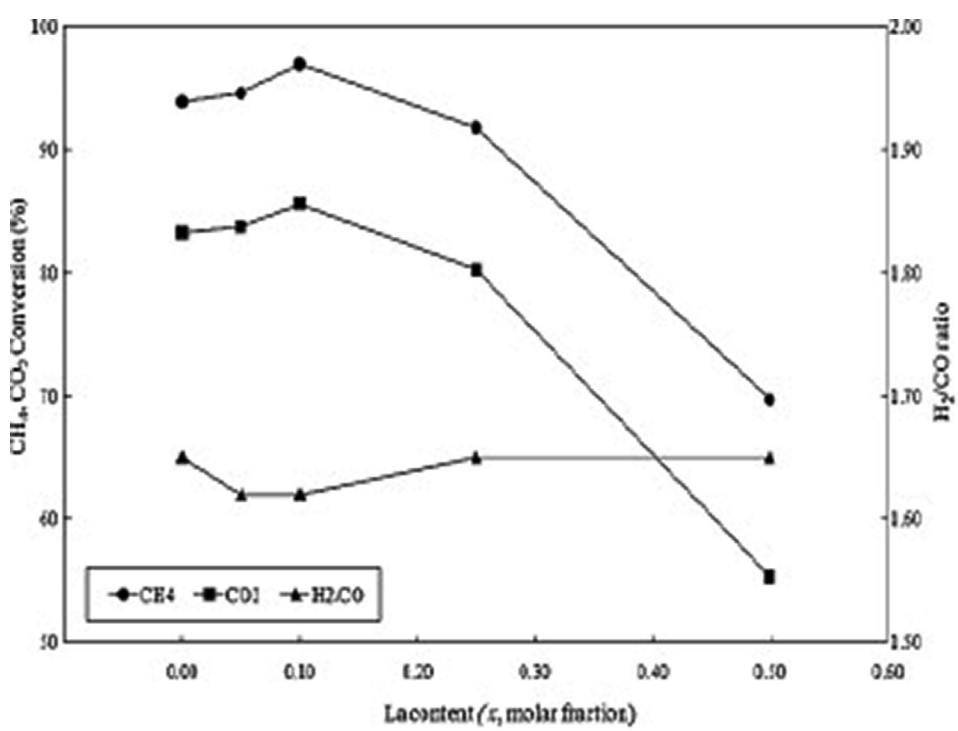

Fig. 6. La effects on performance in the tri-reforming of CH_4 (Pino et al., 2011).

Table 7
TPR analysis showing the H_2 consumption of the synthesized catalysts (Lino et al., 2019).

Sample	Consumption Of H_2 (±5μmol)	consumption of H_2 by Ni species (±5μmol)	H_2 consumption if all Ni° is reduced (±5μmol)	Ni wt% from EDS	Ni reducibility (%)	Weak (%)	Moderate (%)	Strong (%)
MA	0	–	–	–	–	–	–	–
NMA	86.4	86.4	78	9.1	100	4.0	32.4	63.6
ZMA	2.1	–	–	–	–	–	–	–
NZMA	82.8	80.7	88	10.4	92	15.5	31.0	53.5
CZMA	3.4	–	–	–	–	–	–	–
NCZMA	75.0	71.6	68	8.0	100	7.7	40.0	52.3
CMA	8.6	–	–	–	–	–	–	–
NCMA	96.1	87.5	78	8.8	100	2.5	17.6	79.9

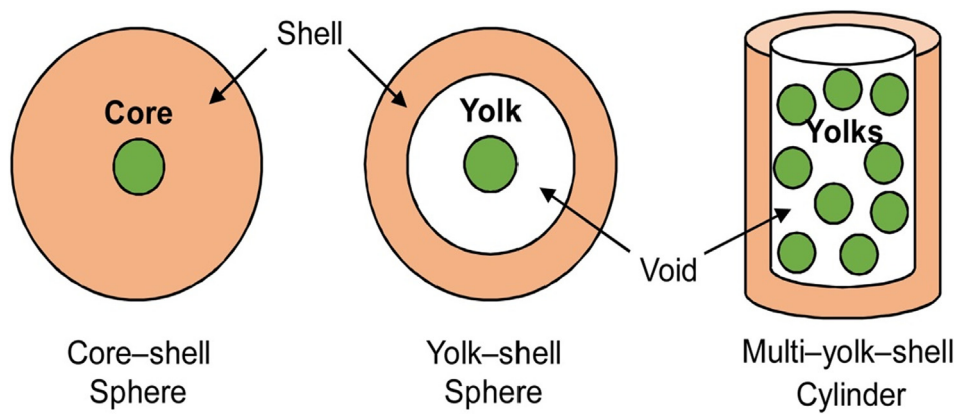

Fig. 7. Core and shell sphere, yolk and shell sphere and multi-yolk and shell cylindrical structures (Kim et al., 2019).

(imp) prepared catalyst. This means that majority of H_2 consumed was by the bulk of NiO coupled with particles of NiO which interacted with CeO_2.

2.4.2. Lanthanide series as support in the tri-reforming of CH_4 (TRM)

The role played by lanthanide series employed as support in TRM was studied by Lee et al. (2004). The performance of three catalysts; Ni/ZrO_2, Ni/Ce-ZrO_2, and Haldor Topose R67-7H were compared. Carbon deposits on the catalysts' surfaces were effectively minimized. More specifically, Ni/Ce-ZrO_2 showed evidence of strong basicity and reduction–oxidation capacity in TRM (Dębek et al., 2015). Ce in the catalyst Ni/Ce-ZrO_2 impacted on the catalyst efficiency by improving the catalyst longevity and increasing the amount of O_2 species mobility. Furthermore, the dependency of carbon formation is tied to the oxidant (steam or O_2) rather than just the strength of the support material, which is in agreement with Kim et al. (2019). In another study where Ce and Zr were utilized for the production of syngas by Walker et al. (2012), the catalyst (Ni-MgO- (Ce, Zr)O_2) parameters such as Ce:Zr ratio, metal loading techniques, metallic wt.% were studied. An even ratio of Ce:Zr and Ni:Mg gave optimum catalyst performance. Embedding ZrO_2 into CeO_2 formed mixed metal oxides which enhanced the capacity to store O_2 and the redox properties of the catalysts (Pérez-Camacho et al., 2014). Upon co-precipitation of the two oxides (ZrO_2 and CeO_2), there were no noticeable ZrO_2 peaks present in the formed support material. All peaks mirrored the cubic structural matrix of pure CeO_2. The catalyst was able to effectively produce the required H_2: CO ratio (2.2) with insignificant amount of deactivation, very good reaction conversion (conversion of CH_4 and CO_2 were 99.6% and 65.6%, respectively) and high stability of the Ni-MgO-(Ce, Zr) O_2 catalyst maintained at the given operating conditions.

Lanthanide series have also been used as bi-metallic supports for several TRM processes. One of such processes was the study by Pino et al. (2014). In their study, Ni catalyst supported on La-Ce-O oxides with varying Ni content were synthesized and used for tri-reforming of simulated biogas. The effect of reactants' ratio on the catalyst productivity was determined. At 800 °C, the catalyst; $Ce_{0.7}La_{0.2}Ni_{0.1}O_{2-\delta}$ had the best performance when biogas to CO_2 ratio was 1.5. CH_4 and CO_2 conversion rates were 1.56 and 0.56 $mmols^{-1}$ g_{Ni}, respectively, while the H_2/CO ratio was 1.57 with no trace of carbon deposited in the 150-h TOS. From the sample analysis carried out, incorporation of Ni and La ions into the CeO_2 structure occurred partially. In addition, the CeO_2 cubic fluorite matrix was not destroyed even at high La doping. Also, the strength of Ni ° and La_2O_3-CeO_2 interaction was reported to be the most significant property responsible for the catalyst's performance (Omoregbe et al., 2016). This interaction between the Ni-La and surface O_2 from Ce enhanced the dispersion of Ni (Usman et al., 2015). LaO species increased the Ni atoms d-electron density,

Table 8
H_2 consumption during H_2-TPR analysis with Ni-Ce-@-SiO_2 multi-York-shell nanotube (^{A} and ^{C} = water to surfactant ratio) and NiCe/SiO_2 impregnation (imp) (Kim et al., 2019).

Catalystssymbol	TotalNi/mmol	H_2 consumptionmmol^{-1}			α/ β
		α	β	γ	
Ni-Ce-@-SiO_2^A	0.07	0.08	0.01	0.02	6.50
Ni-Ce@-SiO_2^C	0.06	0.06	0.01	0.01	7.00
Ni-Ce/Si-O_2^{imp}	0.05	0.02	0.06	0.00	0.30

hence, inhibiting the deposition of carbon. High loading of Ni and La can promote metal sintering, re-oxidation of Ni sites and cover the La species, thereby deactivating the catalyst.

In this sub-section we have identified some literature where lanthanide series have been applied as catalyst/promoter and support for partial oxidation of CH_4. Table 9 represents a summary of selected literature reviewed in this section.

2.5. Lanthanide series in autothermal reforming of CH_4 (ATRM)

2.5.1. Lanthanide series as catalyst/promoter in the autothermal reforming of CH_4 (ATRM)

The application of lanthanide series as catalyst/promoter in the ATRM by various researchers has been outlined in this section. In one of such report by Akri et al. (2016), several Ni-Ce on illite clay with varied Ce loading were employed as catalysts in the ATRM. Adding O_2 to the reactant affected the reaction process due to the carbon imbalance observed when compared with the CH_4/CO_2 mixture (Enger et al., 2009). Also, addition of Ce significantly impacted on the specific surface area due to the improved *meso*-porosity observed (Gallego et al., 2009). For the Ni metal particles, they diminished in size because of the presence of Ce. This led to a new Ni particle size of 16.3 nm from an initial value of 34.2 nm for 10Ni and 10Ni-15Ce. The optimum catalyst performance (observed in the catalyst with 15 wt% Ce) was attributed to the reduction–oxidation ability of the promoted catalyst coupled with the improved dispersion of Ni due to the presence of Ce promoter. Addition of Ce varied directly with the shift in NiO peak to lower temperature. The enhancement effect of Ce on NiO reduction is as a result of Ce^{3+}/Ce^{4+} reduction–oxidation cycle which allowed the transfer of electron to favor the reduction of the NiO species (Daza et al.,

Table 9
Lanthanide series in tri-reforming of CH_4.

Reforming processes	Catalyst type	Lanthanide series	Function of lanthanide series	Aim of study	Outcome of study	References
Tri -reforming of CH_4	Ni-CeO_2	La and Ce	PromoterAnd support	Synthesize and test catalyst in TRM	• 10 wt% of La significantly improved conversion from 93% and 83% to 96% and 86.5% of CH_4 and CO_2, respectively. • Improved basicity	(Pino et al., 2011)
	Ni Catalysts supported on $MgAl_2O_4$	Ce	Promoter	Catalytic test	• Promoted catalyst minimized carbon deposition • Improved conversion of reactants • Reaction with Unpromoted catalyst formed filamentous carbon which cause catalytic instability during reaction • Promoters aided the modification of the catalyst's basic sites component	(Lino et al., 2019)
	Ni and Rh-Ni catalyst on Mg alumina promoted on ZrO_2	CeO_2	Promoter	Improving Hydrogen production from biogas	• Ni-Ce-Zr-Al_2O_3 catalysts produced the highest amount of H_2 • Improved Ni dispersion	(Izquierdo et al., 2013)
	York NiCe@SiO_2 multi-York shell nanotube	CeO_2	Catalyst / promoter	Synthesis and catalytic test	• NiCe/SiO_2 prepared by impregnation technique showed lesser stability than Ni-Ce-@S-iO_2 multi-York shell • NiCe@SiO_2 with yolks less than 20 nm showed better carbon resistance when compared with Ni-Ce-@-SiO_2 with larger sized yolks • Ni-Ce-@SiO_2 with larger sizes were more stable in the TRM	(Kim et al., 2019)
	Ni-based catalyst(Ni/ZrO_2, Ni/Ce-ZrO_2, and Haldor Topose R67-7H)	Ce	Support	Comparison of catalyst	• Carbon deposit was minimized and improved catalytic performance • Improved longevity of Ni/Ce-ZrO_2 • Carbon formation is related to the oxidant in reforming process	(Lee et al., 2004)
	Ni-MgO-(Ce,Zr)O_2	Ce	Support	Effects of catalyst metallic ratio and preparation method	• Optimum performance when using even ratio of catalyst and support material • Wet impregnation method reduced coking more than the precipitation technique • Insignificant amount of deactivation • High catalyst conversion and stability	(Walker et al., 2012)
	Ni catalyst	La-Ce-O oxides	Support	Synthesis and effects of catalyst ratio on the catalyst performance	• $Ce_{0.7}La_{0.2}Ni_{0.10}O_{2-\delta}$ had the best performance • CH_4, CO_2 conversion rates were 1.56 and 0.56 $mmols^{-1}g_{Ni}$, respectively • while the H_2/CO ratio was 1.57 • No trace of carbon deposited in a 150-h reaction span • strong links between the Ni^o and La_2O_3-CeO_2 resulted in good catalytic performance • High loading of Ni and La can promote metal sintering, thereby deactivating the catalyst	(Pino et al., 2014)

2010). Another study utilizing Ni as catalyst and Ce as promoter was reported by Sepehri and Rezaei (2017). In their investigation, they used Ni catalyst and tried to find out the effects of adding trace amount of Ce on Al_2O_3 support. Ni on Ce-Al_2O_3 (Ce- 3 wt%) showed better activity in relation to the Ni on Al_2O_3 and catalyst promoted with 1 wt% and 6 wt% of Ce. Significant stability was also experienced during a 20 h longevity test. In addition, the Ni catalyst on Ce-Al_2O_3 (3 wt%) had the best resistance to carbon, thereby positively altering the autothermal reforming process. Furthermore, adding Ce increases the surface area and catalyst promoted with 3 wt% Ce and 6 wt% Ce improved the NiO dispersion by relocating other species of Ni to $NiAl_xO_y$ species, while Ce (1 wt%) enhanced the catalyst reduction ability as evident in the TPR profile represented in Fig. 8. The profiles revealed two major peaks at temperature of about 450 °C (Kim et al., 2005) and 890 °C (Damyanova and Bueno, 2003). The former peak is assigned to the bulk NiO (Kim et al., 2005), while the later is reduced into three segmented components namely: the reduction of weak Ni^{2+} ions with Al_2O_3 (Patcas and Hönicke, 2005), reduction of Ni^{2+} linked with the non-stoichiometric $NiAl_xO_y$ species and the stoichiometric $NiAl_2O_4$ species (Juan-Juan et al., 2009). Worthy of note was the shift in the reduction peaks towards the NiO-Al_2O_3 species with no changes seen in $NiAl_2O_4$. This is indicative of the interaction between Ni and Ce, thereby making the interaction between the support and Ni easily achievable, hence, enhancing reducibility (Iriondo et al., 2010). According to the authors, the elevated reduction temperature species were related to the uniformly dispersed NiO.

Lanthanide series can be used as catalyst/promoter by combining metals on support. In one of such studies, $NiCoMgO_x$ and $NiCoMgCeO_x$ on Zirconia-haffnia (Ni-Co-Mg-Ce = 1/0.2/1.2/1.2) catalysts were tested in ATRM by Choudhary et al. (2005). Upon increasing the temperature of the reaction to over 2000 °C for 0.5 hr, the catalyst remained stable for all processes with conversion of reactants not altered by the temperature change. When the catalyst sample without CeO_2 was tested at elevated temperature, similar catalyst activity was observed in the partial oxidation of CH_4; however, reduced activity was noticed in CRM and SRM. The superiority of the catalyst with CeO_2 in steam and CO_2 reforming reactions is ascribed to the incorporation of CeO_2 which is rich in O_2 and has the ability to improve the O_2 lattice mobility present in the catalyst matrix (Sutthiumporn et al., 2012), (Choudhary et al., 2005).

Apart from Ni catalyst, other catalysts have been employed for the ATRM. For example, Ni et al., (2014a) synthesized Rh/Al_2O_3 catalysts and promoted with Ce-LaOx , Ce-GdOx, Ce-ZrOx, and Ce-SmOx. Addition of Ce-ZrO_x reduced CO in the product stream. With the ratio of Ce/Zr equal 1:1, a catalyst with the ability to remain stable and active at high temperature was obtained. The effects of adding CeO_2 on conversion of CH_4 and concentration of CO is shown in Fig. 9. In addition, after several test, they obtained an optimized catalyst 0.1%-Rh-2%-MgO-40%-$Ce_{0.5}Zr_{0.5}O_2$-Al_2O_3 which was then analyzed for its stability and compared with the unpromoted Rh-Al_2O_3. The longevity study was carried out for over 80 h TOS and the result was compared to results obtained from 0.1Rh-Al_2O_3 which was tested for 50 h. For the promoted catalysts, deactivation trend was insignificant as compared to the steep deactivation observed in the result from the longevity test carried out with the 0.1% Rh/Al_2O_3 catalyst. The changes in catalysts behavior was attributed to the addition of Ce-Zr and MgO species to the 0.1% Rh/Al_2O_3 catalyst (Ni et al., 2014a). According to the reduction analysis, new species of Rh-oxides were formed. Weak peaks at around 200 °C occurred for the Rh_2O_3-Al_2O_3, which could have been due to the interaction between Rh and Al occurring at various points up to 550 °C. The strong links existing between the oxides of Rh and Al which led to the formation of $RhAlO_3$ was ascribed to the peak present at 700 °C (Fornasiero et al., 1995). When the catalyst was promoted with $Ce_{0.5}Zr_{0.5}O_2$ and MgO, the peak at 700 °C completely fades off indicating the suppression of the strong links between Rh and Al_2O_3. Furthermore, reduction peaks observed at 900 °C was ascribed to the overall bulk reduction of CeO_2 to form the interaction of Ce-Zr which existed in the mixed metallic oxides. In addition, the broad peaks observed between 160 and 560 °C in Rh_2O_3-MgO-$Ce_{0.5}Zr_{0.5}$-Al_2O_3 catalyst is linked to the oxides of Ce-Zr and Rh, respectively. The improved catalyst increased the movement of O_2 in the catalyst resulting in enhanced performance during the ATRM.

2.5.2. Lanthanide series as support in the autothermal-reforming of CH_4

Researchers have also used lanthanide series as support for CH_4 autothermal reforming. In one of such investigations, various load-

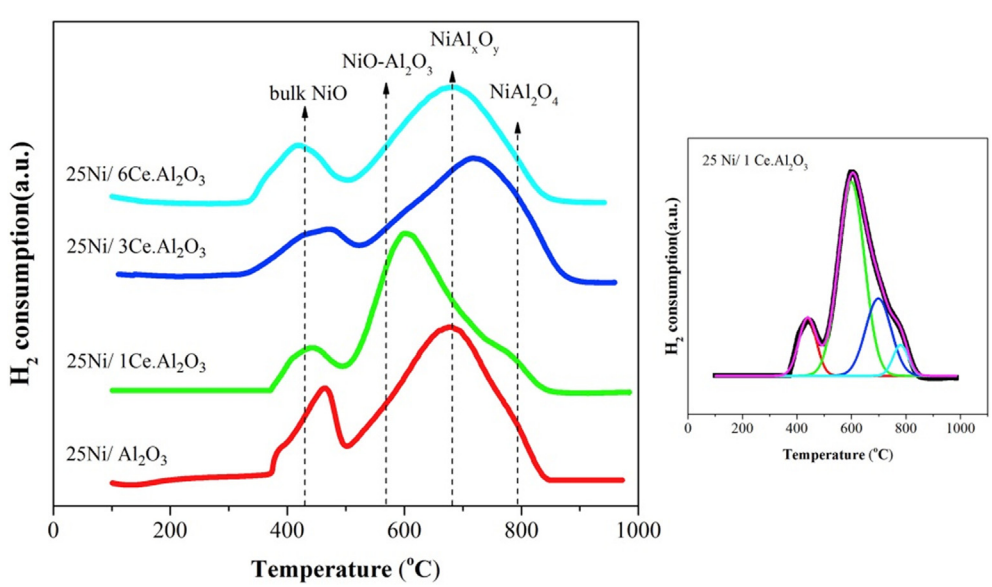

Fig. 8. H_2 consumption vs temperature profile of catalyst samples (Sepehri and Rezaei, 2017).

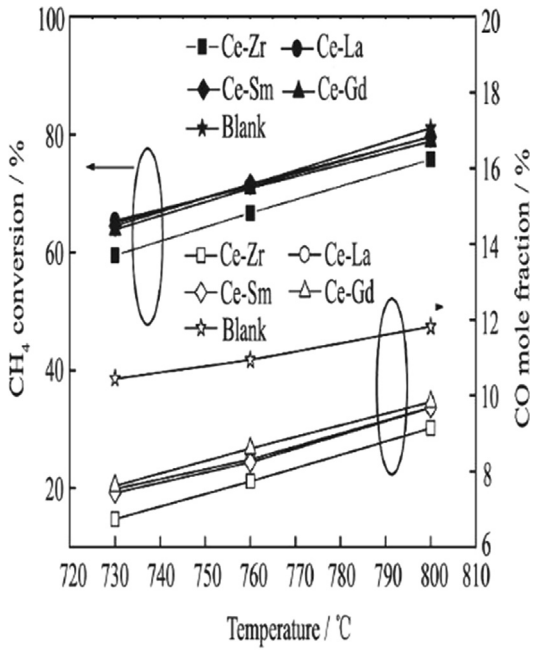

Fig. 9. Conversion / CO mole fraction versus temperature: catalytic effect of adding Ce-based oxide (NI et al., 2014a).

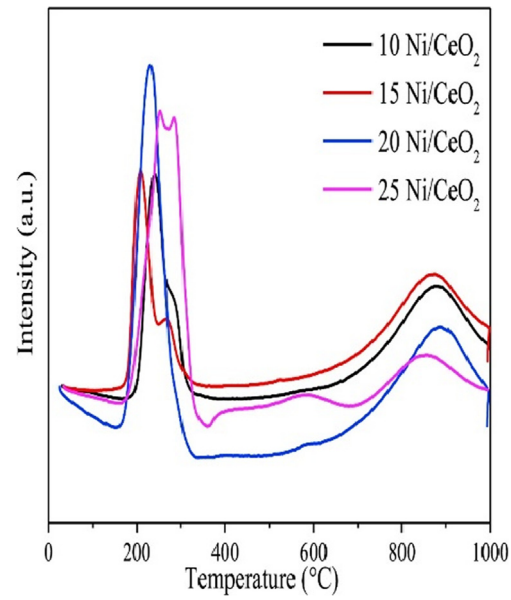

Fig. 10. Spent Ni/CeO_2 catalysts using TPH analysis (Sepehri et al., 2018).

ings of Ni (10, 15, 20 and 25) on Ni-CeO_2 were utilized in the ATRM by Sepehri et al. (2018). The characterizations of the catalyst pre and post reaction were obtained to analyze the catalytic behavior of Ni-CeO_2. From all the catalyst prepared, 20 wt% Ni-CeO_2 was the optimum in terms of activity (over 60% conversion at 700 °C), while 25 wt% Ni-CeO_2 had the best H_2 selectivity. The catalyst efficiency was tied to the high metal dispersion (Khajeh Talkhoncheh and Haghighi, 2015), the specific surface area of CeO_2 (Natesakhawat et al., 2005) and the effectiveness of the support in enhancing the reduction of Ni particles (Chen et al., 2013). Upon investigation of the longevity, the catalyst was stable for the first 10 h and a gradual deactivation commenced afterwards. The deactivation was attributed to the Ni nanoparticles sintering. To confirm this, TPH analysis was carried out on the spent catalyst to ensure the deactivation was not as a result of carbon formation. Interestingly, the results represented in Fig. 10 shows no carbon was deposited on the 20Ni-CeO_2 catalyst. Peaks centered around 200 – 250 °C depicted high reactive carbon species which were converted in-situ reaction (Mirodatos et al., 1987). For the 25 wt % Ni/CeO_2 catalyst, a broad peak representing inactive carbon on the metal surface was located at around 400 – 680 °C (Mirodatos et al., 1987), while the peak at 900 °C was ascribed to CeO_2 reduction. The major reason for the inability of carbon to remain as a single element but rather is converted to useful compounds is the presence of CeO_2 which provides a support platform with sufficient surface area for the dispersion of metallic Ni°. In addition, CeO_2 affinity for acidic CO_2 due its high basicity allows for the formation of carbonate species which cleans carbon off the catalyst surface.

A different type of catalyst (Pt catalysts and support) was used by Ruiz et al. (2008) for ATRM. In order to cleanse carbon from the catalyst surface more effectively, they performed ATRM using various ratio of $CeZrO_2$ support on platinum catalyst. From their study, the best catalyst in terms of stability was found to be Pt/$Ce_{0.75}$-$Zr_{0.25}O_2$. The catalyst ability to remain stable even at elevated temperature was linked to the amount of O_2 vacancies in the support material and the catalyst particle size (Goula et al., 2017). The unique property of the optimal catalyst was its ability to be reduced by the support (Shan et al., 2003), (Branco et al., 2008). In addition, its enhanced O_2 storage capacity aided the uninterrupted cleansing of carbon deposits from the catalyst active site by simple oxidation technique. Other factors which influenced the catalyst behavior were: molar ratio of H_2O/CH_4 which increased CH_4 conversion and ratio of syngas, adding CO_2 to reactants and alteration of the reaction temperature. In this sub-section we have identified few literatures where lanthanide series have been applied as catalyst/promoter and support for partial oxidation of CH_4. Table 10 represents a summary of selected literature reviewed in this paper.

3. The role of lanthanides series on the reaction mechanism, kinetics and carbon formation.

A major variable in methane reforming processes that controls the rate of conversion and formation of carbon species is the intrinsic chemical reaction kinetics which is determined by the mechanism of the reaction. Researchers have attempted to postulate various reaction mechanisms and fit experimental data into existing kinetic models. In relation to lanthanide series as catalyst/promoter or support some studies on the mechanism, kinetics and carbon formation have been reported. In one of such studies, the mechanism and kinetic study of CRM using Pr_2O_3-supported Co catalysts was investigated by Ayodele et al., (2017). In order to reduce the effect of carbon deposits on the reaction carried out at temperature of 750 °C, the experimental data was fitted into several Langmuir-Hinshelwood (LH) models. Consequently, the best fit was a double step dual site model with activation of CH_4 by Co to form H_2 and carbon (Gallego et al., 2008). Furthermore, carbon was gasified by the lattice oxygen from Pr_2O_3 during the activation of CO_2 which is adsorbed on the support site (Pakhare et al., 2014), (Moradi et al., 2010). Oxides of lanthanide series such as Pr_2O_3 have been reported to have very good capacity to store oxygen thereby producing highly mobile oxygen species on the catalyst surface (Harshini et al., 2014). The obtained activation energies for CH_4 and CO_2 were 61.67 and 32.52 kJ mol^{-1}, respectively, indicative of lower energy barriers for CO_2 activation than CH_4.

Using a different type of catalyst, Pakhare et al., (2014) investigated the mechanism and kinetics of CRM using Rh substituted $La_2Zr_2O_7$ pyrochlores catalyst. The catalyst's activity site for CH_4

Table 10
Lanthanide series in autothermal reforming of CH_4 (ATRM).

Reforming processes	Catalyst type	Lanthanide series	Function of lanthanide series	Aim of study	Outcome of study	References
ATRM	Ni-Ce catalysts on illite clay	Ce	Catalyst	Catalytic test	• Addition of Ce reduced the Ni particle size from • 15 wt% Ce catalysts gave the optimum performance • Addition of Ce reduced the temperature of NiO peak in the TPR analysis which minimizes the amount of carbon deposited.	(Akri et al., 2016)
	Ni/Al_2O_3	CeO_2	Promoter	Effect of doping	• 3 wt% Ce-Al_2O_3 showed better activity than Ni/Al_2O_3 • 3 wt% Ce-Al_2O_3 catalyst was stable over a 20 h test time • Improved Ni dispersion	(Sepehri and Rezaei, 2017)
	NiCoMgOx and NiCoMgCeOx supported on Zirconia-haffnia	CeO_2	Catalyst/ promoter	Catalyst behavior	• 98% conversion of reactants • 95% selectivity of products • High temperature up to 2000 °C did not alter the catalyst activity • Catalyst without CeO_2 showed reduced activity for steam and CRM.	(Choudhary et al., 2005)
	Rh/Al_2O_3 catalysts	Ce-GdOxCe-ZrOx, Ce-SmOx, Ce-LaOx,	Promoters	Synthesis and catalytic test	• Addition of Ce-ZrO_x reduced CO in the product stream. • Ce/Zr with ratio 1:1 remained stable and active at high temperature • 0.1-Rh-2.0-MgO-40-$Ce_{0.5}Zr_{0.5}O_2$-Al_2O_3 was the optimum catalyst • when compared to Rh-Al_2O_3, 0.1-Rh-2.0-MgO-40-$Ce_{0.5}Zr_{0.5}O_2$-l_2O_3 catalyst had better resistance to deactivation.	(NI et al., 2014a)
	Ni/CeO_2 catalyst	CeO_2	Support	Catalyst behavior	• 20 wt%Ni/CeO_2 showed best activity • 25 wt% Ni/CeO_2 had the best H_2 selectivity • The support enhanced the high metal dispersion, surface area of CeO_2 and reducibility of the metal particles. • Deactivation of catalyst due to sintering was observed after the first 10 h of reaction.	(Sepehri et al., 2018)
	Pt catalyst on $CeZrO_2$ support	CeO_2	Support	Carbon cleansing from catalyst surface	• $Pt/Ce_{0.75}Zr_{0.25}O_2$ showed the best stability • The $CeZrO_2$ support had high ability to reduce the Pt oxide.	(Ruiz et al., 2008)

and CO_2 activation and their roles in determining the mechanism of CRM was reported. The kinetic rate equation postulated was a dual site mechanism, meaning the activation of the reactants (CH_4 and CO_2) occurred at different sites. Out of all kinetic models tested, two models showed good fit with the data from this study. The activation of CH_4 and CO_2 were the rate determining step for the two different models, respectively. Furthermore, the basic nature of La-O sites activates the acidic CO_2 to yield carbonate complexes (Zhang and Verykios, 1996a). However, CH_4 activation and dissociation site was the Rh site which was verified by transient pulsing of CH_4 on the carbonates. The apparent activation energy for CH_4 and CO_2 obtained in the temperature range 520–605 °C was 21.8 and 18.7 kCal mol^{-1}, respectively. Results from other studies in literature showed that Rh supported catalyst had activation energy of 21.8 and 11.8 kCal mol^{-1} (Múnera et al., 2007), and 22 and 19.28 kCal mol^{-1} (Ghelamallah and Granger, 2012), respectively.

The kinetic study of CRM on promoted (with Ce) and unprompted Ni/Al_2O_3 was studied by Foo et al., (2011a). The study revealed an insignificant change in activation energy and reaction rate of CH_4 (less than 5% increment). However, Ce promoted Ni/Al_2O_3 had better resistance to carbon deposit on the catalyst surface attributable to the equilibrium between various oxidation states of Ce ions. Consequently, two carbon types emerged; C_α and C_β. C_α is removed by H_2 and CeO_2 during redox reaction, while non-reactive C_β is removed by O_2. A dual site Langmuir-Hinshelwood model was postulated with activation energy of 56.40 kJ mol^{-1} and 54.52 kJ mol^{-1} for the un-promoted and promoted catalyst, respectively.

The kinetics of CRM over Ni/La_2O_3 at temperature of 750 °C have been investigated by Tsipouriari and Verykios, (2001). The mechanism steps involves adsorption of CH_4 on the metallic site, CH_4 cracking and deposition of carbon. The controlling step was the CO_2 reaction with La_2O_3 which formed carbonates that reacted with carbon at the catalyst surface. The kinetic model of Ni/La_2O_3 suggests that more stable catalyst sites are formed on the catalyst surface in-situ reaction, thereby leading to the adoption of the mechanism used previously in literature (Zhang and Verykios, 1996b), (Zhang and Verykios, 1996a) which postulated similar behavior.

Another study using similar catalyst was investigated by Slagtern et al., (1997). In the study, the mechanism of CRM over Ni/La_2O_3 was studied using the transient kinetic experiment and comparison was made with the conventional Ni catalyst. The existence of a close interaction between the Ni particles and the in-situ formulated carbonate phase was essential for the reaction process. Dual functional mechanism translates to the eventual kinetic behavior where CH_4 activation occurs on the Ni particles and CO_2 interaction is on the La_2O_3 forming carbonates. This La carbonate species reacts with carbon at the catalyst interface thereby removing carbon species from the metallic phase. In addition, the morphological structure of the existing active phase had an impact in hindering carbon deactivation which translates to a very stable catalyst. Similar mechanism and kinetic have been reported in existing literature (Gallego et al., 2008), (Mu et al., 2007). In the study by (Gallego et al., 2008), when compared with literature for noble metal catalyst, Ni/La_2O_3 catalyst (from $LaNiO_3$) performed better using similar mechanism to obtain lower activation

energies. Activation energies of CH_4 and CO_2 at 973 K were 68 and 77 kJmol^{-1}, respectively, surpassing the performance of noble metal catalyst which gave activation energy values of between 83 and 125 kJ mol^{-1} (Erdohelyi et al., 1993). The rate controlling step was considered to be the CH_4 cracking on the metallic nickel particles to yield carbon. CO_2 is subsequently adsorbed by La_2O_3 to yield its carbonate which then reacts with carbon at the interface to produce CO and clean up the metal surface.

The kinetics of steam reforming of methane over Rh/$Ce_\alpha Zr_{1-\alpha}O_2$ catalyst was reported by Halabi et al., (2010a). The activation energy for the steam reforming process was 83.8 kJ mol^{-1} which was comparable to activation energy of Rh catalyst supported on Gd promoted CeO_2 (92 kJ mol^{-1}) (Hennings and Reimert, 2008) and Rh on Al_2O_3 (109 kJ mol^{-1}) (Wei and Iglesia, 2004). Lower activation energy observed for the Rh/$Ce_\alpha Zr_{1-\alpha}O_2$ catalyst can be linked to the metal support interaction. Furthermore, a dual site adsorption surface hypothesis alongside 14 basic reaction steps was adopted. According to the model, CH_4 is adsorbed on the metal sites while steam is adsorbed on the CeO_2 support site. This means that there was no competition between the reactants adsorbing on the same site. Additionally, the kinetic rate of reaction model adopted was according to Langmuir-Hinshelwood expression. CeO_2 was responsible for the rate controlling step as it provided sufficient lattice oxygen which gasified the carbon species to form CO and CO_2.

Also, studies have been carried out attempting to develop a substantial mechanism for the formation of carbon in CH_4 reforming processes when lanthanide series were used. In a study by Wang et al., (2006), the metal support interaction between Rh and CeO_2 in the catalyst Rh-CeO_2/Al_2O_3 for CRM was reported by Wang et al., (2006). Carbon formation on Rh/Al_2O_3 was resisted by promoting with CeO_2. Following the reaction mechanism, dissociation of reducing agents H_2 and CH_4 is activated on the metallic site, thereby freeing electrons to attack the CeO_2 which is in close interaction with the metal forming Ce^{4+}/Ce^{3+} and $Rh^{\circ}/Rh^{\delta+}$ couples (Bernal et al., 1999). The activation of the reactants; CH_4 and CO_2 is carried out by these couples, with the Ce^{4+}/Ce^{3+} couple responsible for the activation of CO_2. Free electrons from Ce^{3+} are responsible for the formation of CO from deposited carbon on the surface.

In another study, Foo et al., (2011b) determined the influence of lanthanide series (Ce, Pr and Sm) on Co-Ni/Al_2O_3 in CRM. Results showed an increase in the rate of production of syngas resulting from usage of carbon species. Carbon deposit was substantially reduced by about 50% with the lanthanide series having a noticeable effect in the order Ce, Pr and Sm at reaction temperature of 700 °C. The study showed that the promoted catalyst's H_2 and CO formation rate constants, coupled with their reaction orders, enthalpy and entropy of CH_4 adsorption were slightly better than that of the un-promoted catalyst. The enhanced behavior is linked to the Pauling's electronegativity of the promoted catalyst. This resulted in the formation of dual carbon species; a reactive species found in the promoted catalyst and an unreactive species which was present in both catalysts (promoted and un-promoted). The kinetic study at 700 °C was also carried out using the Langmuir Hinshelwood model with both promoted and un-promoted catalysts having similar activation energy values of about 47 kJ mol^{-1}.

Nonetheless, carbon species and carbon formation on supported metals are moderately understood. Carbon structures of varying carbon species need to be well defined. Several literatures have attempted to establish relationships between the quantity of carbon deposited on catalyst surface and the extent of catalyst deactivation. More rate data are required for these steps which entails the formation of various types of carbon molecules for various methane reforming processes. Increased data will provide better understanding of the basic fundamentals for developing more effective catalyst that can withstand severe deactivation and subsequently increase productivity.

4. Conclusions

The need to substitute the depleting fossil fuel reserves and to switch to clean fuel from natural gas reserves is now becoming a reality. Also, the utilization of biogas from decomposing organic biomass which is high in CH_4 and CO_2 (two major environmental pollutant) is of great interest. A technique to utilize CH_4 effectively is to carry out its reforming with reactants such as steam, O_2 and CO_2 to form more valuable products like H_2 and syngas. Several researchers have achieved scintillating outcomes from trials of these reforming techniques as reported in this comparative study. However, a common setback in CH_4 reforming processes is the formation of substantial amount of carbon enough to halt the reaction process. Researchers have tried to eliminate carbon by introducing specific catalysts which alters the reforming reaction pathway. According to existing literatures which have been extensively reviewed in this paper, lanthanide series play a major role in formulating a befitting catalyst that can effectively minimize carbon formation during any form of reforming process. Specific qualities such as improved basicity, reduction - oxidation properties, high O_2 mobility and storage capacity are some of the properties of the lanthanide series which have altered the reaction pathways and enhanced the longevity of the reforming reaction. Some of the catalyst's properties altered by the lanthanide series include: the reducibility (identified by TPR), pore volume (identified by N_2 physisorption), crystalline structure/size (identified by XRD) and the catalyst morphology (identified by TEM and FESEM). Also, worthy of note is the use of lanthanide series as support or promoter in steam reforming of CH_4 (SRM) to effectively eliminate by-products (carbon and CO_2) which are major challenges in the SRM.

Lanthanide series have also played key roles in the mechanism and kinetics of CH_4 reforming reactions by taking part in the rate determining step. Hence, they are mainly involved in the removal of carbon species since the formation of carbon is a key step in CH_4 reforming processes. However, the formation of carbon species on catalyst materials is a complex process. Attempts have been made to establish the relationships between deactivation and the amount of carbon on catalyst surfaces. Moreover, specific rate data are needed for these steps as this would provide the fundamental data required to formulate and commercialize highly resistant catalysts that can withstand deactivation. Hence, this study is beneficial for sustaining the life of an industrial catalyst over time as it brings together comparative data on the role of lanthanide series in CH_4 reaction over various reforming processes.

Declaration of Competing Interest

The authors declared that there is no conflict of interest.

Acknowledgement

Osarieme Uyi Osazuwa is a recipient of Universiti Malaysia Pahang Post-Doctoral Fellowship in Research.

References

Abdollahifar, M., Haghighi, M., Babaluo, A.A., 2014. Syngas production via dry reforming of methane over Ni/Al2O3–MgO nanocatalyst synthesized using ultrasound energy. J. Ind. Eng. Chem. 20, 1845–1851. https://doi.org/10.1016/J.JIEC.2013.08.041.

Abdullah, B., Abd Ghani, N.A., Vo, D.V.N., 2017. Recent advances in dry reforming of methane over Ni-based catalysts. J. Clean. Prod. https://doi.org/10.1016/j.jclepro.2017.05.176.

Abdullah, N., Ainirazali, N., Chong, C.C., Razak, H.A., Setiabudi, H.D., Chin, S.Y., Jalil, A. A., 2019. Effect of Ni loading on SBA-15 synthesized from palm oil fuel ash

waste for hydrogen production via CH4 dry reforming. Int. J. Hydrogen Energy. https://doi.org/10.1016/J.IJHYDENE.2019.09.093.
Akbari, E., Alavi, S.M., Rezaei, M., 2018. CeO2 Promoted Ni-MgO-Al2O3 nanocatalysts for carbon dioxide reforming of methane. J. CO2 Util. https://doi.org/10.1016/j.jcou.2017.12.015.
Akri, M., Chafik, T., Granger, P., Ayrault, P., Batiot-Dupeyrat, C., 2016. Novel nickel promoted illite clay based catalyst for autothermal dry reforming of methane. Fuel. https://doi.org/10.1016/j.fuel.2016.03.018.
Al-Fatesh, A.S., Naeem, M.A., Fakeeha, A.H., Abasaeed, A.E., 2014. Role of La2O3 as promoter and support in Ni/γ-Al2O3 catalysts for dry reforming of methane. Chinese J. Chem. Eng. https://doi.org/10.1016/S1004-9541(14)60029-X.
Al-Musa, A., Al-Saleh, M., Ioakeimidis, Z.C., Ouzounidou, M., Yentekakis, I.V., Konsolakis, M., Marnellos, G.E., 2014. Hydrogen production by iso-octane steam reforming over Cu catalysts supported on rare earth oxides (REOs). Int. J. Hydrogen Energy 39, 1350–1363. https://doi.org/10.1016/J.IJHYDENE.2013.11.013.
Ali, S., Al-Marri, M.J., Abdelmoneim, A.G., Kumar, A., Khader, M.M., 2016. Catalytic evaluation of nickel nanoparticles in methane steam reforming. Int. J. Hydrogen Energy 41, 22876–22885. https://doi.org/10.1016/J.IJHYDENE.2016.08.200.
Alipour-Dehkordi, A., Khademi, M.H., 2020. O2, H2O or CO2 side-feeding policy in methane tri-reforming reactor: The role of influencing parameters. Int. J. Hydrogen Energy. https://doi.org/10.1016/j.ijhydene.2020.03.239.
Alipour, Z., Rezaei, M., Meshkani, F., 2014. Effect of alkaline earth promoters (MgO, CaO, and BaO) on the activity and coke formation of Ni catalysts supported on nanocrystalline Al2O3 in dry reforming of methane. J. Ind. Eng. Chem. 20, 2858–2863. https://doi.org/10.1016/J.JIEC.2013.11.018.
Amin, M.H., Putla, S., Hamid, S.B.A., Bhargava, S.K., 2015. Understanding the role of lanthanide promoters on the structure-activity of nanosized Ni/γ-Al2O3 catalysts in carbon dioxide reforming of methane. Appl. Catal. A Gen. https://doi.org/10.1016/j.apcata.2014.12.038.
Anchieta, C.G., Assaf, E.M., Assaf, J.M., 2019. Effect of ionic liquid in Ni/ZrO 2 catalysts applied to syngas production by methane tri-reforming. Int. J. Hydrogen Energy. https://doi.org/10.1016/j.ijhydene.2019.02.122.
Aneggi, E., Boaro, M., de Leitenburg, C., Dolcetti, G., Trovarelli, A., 2006. Insights into the dynamics of oxygen storage/release phenomena in model ceria–zirconia catalysts as inferred from transient studies using H2, CO and soot as reductants. Catal. Today 112, 94–98. https://doi.org/10.1016/J.CATTOD.2005.11.019.
Anjaneya, K.C., Manjanna, J., Nayaka, G.P., Ashwin Kumar, V.M., Govindaraj, G., Ganesha, K.N., 2014. Citrate-complexation synthesized Ce0.85Gd0.15O2−δ (GDC15) as solid electrolyte for intermediate temperature SOFC. Phys. B Condens. Matter 447, 51–55. https://doi.org/10.1016/J.PHYSB.2014.04.056.
Araujo, G.C. de, Lima, S.M. de, Assaf, J.M., Peña, M.A., Fierro, J.L.G., do Carmo Rangel, M., 2008. Catalytic evaluation of perovskite-type oxide LaNi1−xRuxO3 in methane dry reforming. Catal. Today 133–135, 129–135. https://doi.org/10.1016/J.CATTOD.2007.12.049.
Arcotumapathy, V., Alenazey, F.S., Al-Otaibi, R.L., Vo, D.-V.N., Alotaibi, F.M., Adesina, A.A., 2015. Mechanistic investigation of methane steam reforming over Ce-promoted Ni/SBA-15 catalyst. Appl. Petrochemical Res. 5, 393–404. https://doi.org/10.1007/s13203-015-0121-2.
Ayodele, B.V., Abdullah, S.B., Cheng, C.K., 2017. Kinetics and mechanistic studies of CO-rich hydrogen production by CH4/CO2reforming over Praseodymia supported cobalt catalysts. Int. J. Hydrogen Energy 42, 28408–28424. https://doi.org/10.1016/j.ijhydene.2017.09.037.
Azizzadeh Fard, A., Arvaneh, R., Alavi, S.M., Bazyari, A., Valaei, A., 2019. Propane steam reforming over promoted Ni–Ce/MgAl2O4 catalysts: Effects of Ce promoter on the catalyst performance using developed CCD model. Int. J. Hydrogen Energy 44, 21607–21622. https://doi.org/10.1016/J.IJHYDENE.2019.06.100.
Barrai, F., Jackson, T., Whitmore, N., Castaldi, M.J., 2007. The role of carbon deposition on precious metal catalyst activity during dry reforming of biogas. Catal. Today 129, 391–396. https://doi.org/10.1016/j.cattod.2007.07.024.
Bedrane, S., Descorme, C., Duprez, D., 2002. Towards the comprehension of oxygen storage processes on model three-way catalysts. Catal. Today 73, 233–238. https://doi.org/10.1016/S0920-5861(02)00005-6.
Bereketidou, O.A., Goula, M.A., 2012. Biogas reforming for syngas production over nickel supported on ceria–alumina catalysts. Catal. Today 195, 93–100. https://doi.org/10.1016/J.CATTOD.2012.07.006.
Berger-Karin, C., Sebek, M., Pohl, M.M., Bentrup, U., Kondratenko, V.A., Steinfeldt, N., Kondratenko, E.V., 2012. Tailored Noble Metal Nanoparticles on γ-Al 2O 3 for High Temperature CH 4 Conversion to Syngas. ChemCatChem 4, 1368–1375. https://doi.org/10.1002/cctc.201200096.
Bernal, S., Calvino, J.J., Cauqui, M.A., Gatica, J.M., Larese, C., Pérez Omil, J.A., Pintado, J.M., 1999. Some recent results on metal/support interaction effects in NM/CeO2 (NM: noble metal) catalysts. Catal. Today 50, 175–206. https://doi.org/10.1016/S0920-5861(98)00503-3.
Bitter, J.H., Seshan, K., Lercher, J.A., 2000. On the contribution of X-ray absorption spectroscopy to explore structure and activity relations of Pt/ZrO2 catalysts for CO2/CH4 reforming. Top. Catal. 10, 295–305.
Boaro, M., de Leitenburg, C., Dolcetti, G., Trovarelli, A., 2000. The Dynamics of Oxygen Storage in Ceria-Zirconia Model Catalysts Measured by CO Oxidation under Stationary and Cycling Feedstream Compositions. J. Catal. 193, 338–347. https://doi.org/10.1006/JCAT.2000.2887.
Bobadilla, L.F., Penkova, A., Álvarez, A., Domínguez, M.I., Romero-Sarria, F., Centeno, M.A., Odriozola, J.A., 2015. Glycerol steam reforming on bimetallic NiSn/CeO2-MgO-Al2O3 catalysts: Influence of the support, reaction parameters and deactivation/regeneration processes. Appl. Catal. A Gen. https://doi.org/10.1016/j.apcata.2014.12.029.
Branco, J.B., Ballivet-Tkatchenko, D., de Matos, A.P., 2008. Reduction and catalytic behaviour of heterobimetallic copper–lanthanide oxides. J. Alloy. Compd. 464, 399–406. https://doi.org/10.1016/J.JALLCOM.2007.10.001.
Branco, J.B., Brito, P.E., Ferreira, A.C., 2020. Methanation of CO2 over nickel-lanthanide bimetallic oxides supported on silica. Chem. Eng. J. 380,. https://doi.org/10.1016/J.CEJ.2019.122465 122465.
Buelens, L.C., Galvita, V.V., Poelman, H., Detavernier, C., Marin, G.B., 2016. Super-dry reforming of methane intensifies CO2 utilization via le Chatelier's principle. Science (80-.). 354, 449–452. https://doi.org/10.1126/science.aah7161.
Buyevskaya, O.V., Wolf, D., Baerns, M., 1994. Rhodium-catalyzed partial oxidation of methane to CO and H2. Transient studies on its mechanism. Catal. Letters 29, 249–260. https://doi.org/10.1007/BF00814271.
Calles, J.A., Carrero, A., Vizcaíno, A.J., 2009. Ce and La modification of mesoporous Cu-Ni/SBA-15 catalysts for hydrogen production through ethanol steam reforming. Microporous Mesoporous Mater. https://doi.org/10.1016/j.micromeso.2008.10.028.
Charisiou, N.D., Siakavelas, G., Papageridis, K.N., Baklavaridis, A., Tzounis, L., Avraam, D.G., Goula, M.A., 2016. Syngas production via the biogas dry reforming reaction over nickel supported on modified with CeO2 and/or La2O3 alumina catalysts. J. Nat. Gas Sci. Eng. https://doi.org/10.1016/j.jngse.2016.02.021.
Cheah, S.K., Massin, L., Aouine, M., Steil, M.C., Fouletier, J., Gélin, P., 2018. Methane steam reforming in water deficient conditions on Ir/Ce0.9Gd0.1O2-x catalyst: Metal-support interactions and catalytic activity enhancement. Appl. Catal. B Environ. 234, 279–289. https://doi.org/10.1016/J.APCATB.2018.04.048.
Chen, W., Zhao, G., Xue, Q., Chen, L., Lu, Y., 2013. High carbon-resistance Ni/CeAlO3-Al2O3 catalyst for CH4/CO2 reforming. Appl. Catal. B Environ. 136–137, 260–268. https://doi.org/10.1016/j.apcatb.2013.01.044.
Chiba, R., Komatsu, T., Orui, H., Taguchi, H., Nozawa, K., Arai, H., 2009. Sofc cathodes composed of la Ni0.6 Fe0.4 O3 and pr-doped Ce O2. Electrochem. Solid-State Lett. 12, 69–72. https://doi.org/10.1149/1.3086726.
Chong, C.C., Teh, L.P., Setiabudi, H.D., 2019. Syngas production via CO2 reforming of CH4 over Ni-based SBA-15: Promotional effect of promoters (Ce, Mg, and Zr). Mater. Today Energy 12, 408–417. https://doi.org/10.1016/J.MTENER.2019.04.001.
Choudhary, V.R., Mondal, K.C., Mamman, A.S., 2005. High-temperature stable and highly active/selective supported NiCoMgCeOx catalyst suitable for autothermal reforming of methane to syngas. J. Catal. 233, 36–40. https://doi.org/10.1016/J.JCAT.2005.04.019.
Choudhary, V.R., Rajput, A.M., Prabhakar, B., 1995. Energy efficient methane-to-syngas conversion with low H2/CO ratio by simultaneous catalytic reactions of methane with carbon dioxide and oxygen. Catal. Letters 32, 391–396. https://doi.org/10.1007/BF00813234.
Craciun, R., Daniell, W., Knözinger, H., 2002. The effect of CeO2 structure on the activity of supported Pd catalysts used for methane steam reforming. Appl. Catal. A Gen. 230, 153–168. https://doi.org/10.1016/S0926-860X(01)01003-1.
Da Silva, A.M., De Souza, K.R., Mattos, L.V., Jacobs, G., Davis, B.H., Noronha, F.B., 2011. The effect of support reducibility on the stability of Co/CeO2 for the oxidative steam reforming of ethanol. Catal. Today. https://doi.org/10.1016/j.cattod.2010.10.033.
Damyanova, S., Bueno, J.M., 2003. Effect of CeO2 loading on the surface and catalytic behaviors of CeO2-Al2O3-supported Pt catalysts. Appl. Catal. A Gen. 253, 135–150. https://doi.org/10.1016/S0926-860X(03)00500-3.
Daza, C.E., Gallego, J., Mondragón, F., Moreno, S., Molina, R., 2010. High stability of Ce-promoted Ni/Mg-Al catalysts derived from hydrotalcites in dry reforming of methane. Fuel. https://doi.org/10.1016/j.fuel.2009.10.010.
Daza, C.E., Moreno, S., Molina, R., 2011. Co-precipitated Ni–Mg–Al catalysts containing Ce for CO2 reforming of methane. Int. J. Hydrogen Energy 36, 3886–3894. https://doi.org/10.1016/J.IJHYDENE.2010.12.082.
de Llobet, S., Pinilla, J.L., Lazaro, M.J., Moliner, R., Suelves, I., 2013. CH4 and CO2 partial pressures influence and deactivation study on the Catalytic Decomposition of Biogas over a Ni catalyst. Fuel 111, 778–783. https://doi.org/10.1016/j.fuel.2013.05.001.
de Rogatis, L., Cargnello, M., Gombac, V., Lorenzut, B., Montini, T., Fornasiero, P., 2010. Embedded phases: A way to active and stable catalysts. ChemSusChem 3, 24–42. https://doi.org/10.1002/cssc.200900151.
Dębek, R., Radlik, M., Motak, M., Galvez, M.E., Turek, W., Da Costa, P., Grzybek, T., 2015. Ni-containing Ce-promoted hydrotalcite derived materials as catalysts for methane reforming with carbon dioxide at low temperature - On the effect of basicity. Catal. Today. https://doi.org/10.1016/j.cattod.2015.03.017
Dedov, A.G., Loktev, A.S., Komissarenko, D.A., Mazo, G.N., Shlyakhtin, O.A., Parkhomenko, K. V., Kiennemann, A.A., Roger, A.C., Ishmurzin, A. V., Moiseev, I.I., 2015. Partial oxidation of methane to produce syngas over a neodymium-calcium cobaltate-based catalyst. Appl. Catal. A Gen. https://doi.org/10.1016/j.apcata.2014.10.027
Dega, F.B., Chamoumi, M., Braidy, N., Abatzoglou, N., 2019. Autothermal dry reforming of methane with a nickel spinellized catalyst prepared from a negative value metallurgical residue. Renew. Energy 138, 1239–1249. https://doi.org/10.1016/J.RENENE.2019.01.125.
Del Angel, G., Guzmán, C., Bonilla, A., Torres, G., Padilla, J.M., 2005. Lanthanum effect on the textural and structural properties of γ-Al2O3 obtained from Boehmite. Mater. Lett. 59, 499–502. https://doi.org/10.1016/J.MATLET.2004.10.033.
Dittmar, B., Behrens, A., Schödel, N., Rüttinger, M., Franco, T., Straczewski, G., Dittmeyer, R., 2013. Methane steam reforming operation and thermal stability

of new porous metal supported tubular palladium composite membranes. Int. J. Hydrogen Energy. https://doi.org/10.1016/j.ijhydene.2013.05.030.
Djaidja, A., Libs, S., Kiennemann, A., Barama, A., 2006. Characterization and activity in dry reforming of methane on NiMg/Al and Ni/MgO catalysts. Catal. Today 113, 194–200. https://doi.org/10.1016/J.CATTOD.2005.11.066.
Duarte, R.B., Olea, M., Iro, E., Sasaki, T., Itako, K., Van Bokhoven, J.A., 2014. Transient mechanistic studies of methane steam reforming over ceria-promoted Rh/Al2O3 catalysts. ChemCatChem 6, 2898–2903. https://doi.org/10.1002/cctc.201402388.
Enger, B.C., Lødeng, R., Holmen, A., 2009. Modified cobalt catalysts in the partial oxidation of methane at moderate temperatures. J. Catal. 262, 188–198. https://doi.org/10.1016/j.jcat.2008.12.014.
Erdohelyi, A., Cserenyi, J., Solymosi, F., 1993. Activation of CH4 and Its Reaction with CO2 over Supported Rh Catalysts. J. Catal. https://doi.org/10.1006/jcat.1993.1136.
Ermakova, M.A., Ermakov, D.Y., Chuvilin, A.L., Kuvshinov, G.G., 2001. Decomposition of Methane over Iron Catalysts at the Range of Moderate Temperatures: The Influence of Structure of the Catalytic Systems and the Reaction Conditions on the Yield of Carbon and Morphology of Carbon Filaments. J. Catal. 201, 183–197. https://doi.org/10.1006/jcat.2001.3243.
Escritori, J.C., Dantas, S.C., Soares, R.R., Hori, C.E., 2009. Methane autothermal reforming on nickel–ceria–zirconia based catalysts. Catal. Commun. 10, 1090–1094. https://doi.org/10.1016/J.CATCOM.2009.01.001.
Fan, M.S., Abdullah, A.Z., Bhatia, S., 2009. Catalytic technology for carbon dioxide reforming of methane to synthesis gas. ChemCatChem 1, 192–208. https://doi.org/10.1002/cctc.200900025.
Fang, X., Zhang, J., Liu, J., Wang, C., Huang, Q., Xu, X., Peng, H., Liu, W., Wang, X., Zhou, W., 2018. Methane dry reforming over Ni/Mg-Al-O: On the significant promotional effects of rare earth Ce and Nd metal oxides. J. CO2 Util. 25, 242–253. https://doi.org/10.1016/J.JCOU.2018.04.011.
Fedorova, Z.A., Danilova, M.M., Zaikovskii, V.I., 2020. Porous nickel-based catalysts for tri-reforming of methane to synthesis gas: Catalytic activity. Mater. Lett. 261,. https://doi.org/10.1016/j.matlet.2019.127087 127087.
Feio, L.S.F., Hori, C.E., Mattos, L.V., Zanchet, D., Noronha, F.B., Bueno, J.M.C., 2008. Partial oxidation and autothermal reforming of methane on Pd/CeO2–Al2O3 catalysts. Appl. Catal. A Gen. 348, 183–192. https://doi.org/10.1016/J.APCATA.2008.06.030.
Ferreira, A.C., Ferraria, A.M., do Rego, A.M.B., Gonçalves, A.P., Correia, M.R., Gasche, T.A., Branco, J.B., 2010a. Partial oxidation of methane over bimetallic nickel-lanthanide oxides. J. Alloys Compd. https://doi.org/10.1016/j.jallcom.2009.09.082
Ferreira, A.C., Ferraria, A.M., do Rego, A.M.B., Gonçalves, A.P., Girão, A.V., Correia, R., Gasche, T.A., Branco, J.B., 2010b. Partial oxidation of methane over bimetallic copper-cerium oxide catalysts. J. Mol. Catal. A Chem. https://doi.org/10.1016/j.molcata.2009.12.014.
Florea, M., Matei-Rutkovska, F., Postole, G., Urda, A., Neatu, F., Pârvulescu, V.I., Gelin, P., 2018. Doped ceria prepared by precipitation route for steam reforming of methane. Catal. Today 306, 166–171. https://doi.org/10.1016/J.CATTOD.2016.12.006.
Foo, S.Y., Cheng, C.K., Nguyen, T.-H., Adesina, A.A., 2011a. Kinetic study of methane CO2 reforming on Co–Ni/Al2O3 and Ce–Co–Ni/Al2O3 catalysts. Catal. Today 164, 221–226. https://doi.org/10.1016/j.cattod.2010.10.092.
Foo, S.Y., Cheng, C.K., Nguyen, T.H., Adesina, A.A., 2011b. Evaluation of lanthanide-group promoters on Co-Ni/Al2O 3 catalysts for CH4 dry reforming. J. Mol. Catal. A: Chem. https://doi.org/10.1016/j.molcata.2011.04.018.
Fornasiero, P., Monte, R. Di, Kaspar, J., Meriani, S., Trovarelli, A., Graziani, M., 1995. Rh-Loaded CeO2-ZrO2 Solid Solutions as Highly Efficient Oxygen Exchangers: Dependence of the Reduction Behavior and the Oxygen Storage Capacity on the Structural Properties. J. Catal.
Gallego, G.S., Batiot-Dupeyrat, C., Barrault, J., Florez, E., Mondragón, F., 2008. Dry reforming of methane over LaNi1−yByO3±δ (B=Mg, Co) perovskites used as catalyst precursor. Appl. Catal. A Gen. 334, 251–258. https://doi.org/10.1016/j.apcata.2007.10.010.
Gallego, S., Batiot-dupeyrat, C., Mondrago, F., 2008. Dual Active-Site Mechanism for Dry Methane Reforming over Ni/La 2 O 3 Produced from LaNiO 3 Perovskite. Ind. Eng. Chem. (Analytical Ed. 47, 9272–9278. https://doi.org/10.1021/ie800281t.
Gallego, G.S., Marín, J.G., Batiot-Dupeyrat, C., Barrault, J., Mondragón, F., 2009. Influence of Pr and Ce in dry methane reforming catalysts produced from La1−xAxNiO3−δ perovskites. Appl. Catal. A Gen. 369, 97–103. https://doi.org/10.1016/j.apcata.2009.09.004.
Galuszka, J., Pandey, R., Ahmed, S., 1998. Methane conversion to syngas in a palladium membrane reactor. Catal. Today 46, 83–89. https://doi.org/10.1016/S0920-5861(98)00329-0.
Ghelamallah, M., Granger, P., 2012. Impact of barium and lanthanum incorporation to supported Pt and Rh on α-Al 2O 3 in the dry reforming of methane. Fuel 97, 269–276. https://doi.org/10.1016/j.fuel.2012.02.068.
Goscianska, J., Pietrzak, R., Matos, J., 2018. Catalytic performance of ordered mesoporous carbons modified with lanthanides in dry methane reforming. Catal. Today 301, 204–216. https://doi.org/10.1016/j.cattod.2017.05.014.
Goula, M.A., Charisiou, N.D., Papageridis, K.N., Delimitis, A., Pachatouridou, E., Iliopoulou, E.F., 2015. Nickel on alumina catalysts for the production of hydrogen rich mixtures via the biogas dry reforming reaction: Influence of the synthesis method. Int. J. Hydrogen Energy. https://doi.org/10.1016/j.ijhydene.2015.05.129.
Goula, M.A., Charisiou, N.D., Siakavelas, G., Tzounis, L., Tsiaoussis, I., Panagiotopoulou, P., Goula, G., Yentekakis, I. V., 2017. Syngas production via the biogas dry reforming reaction over Ni supported on zirconia modified with CeO2 or La2O3 catalysts. Int. J. Hydrogen Energy. https://doi.org/10.1016/j.ijhydene.2016.11.196.
Gronchi, P., Centola, P., Rosso, R.D., 1997. Dry reforming of CH4 with Ni and Rh metal catalysts supported on SiO2 and La2O3. Appl. Catal. A Gen. 152, 83–92. https://doi.org/10.1016/S0926-860X(96)00358-4.
Gubareni, I.V., Soloviev, S.O., Kurylets, Y.P., Kapran, A.Y., 2018. Steam and steam-oxygen reforming of methane on NiAl2O3–MxOy (M: La, Ce) based monoliths: effects of catalyst and reaction mixture composition. React. Kinet. Mech. Catal. 123, 641–658. https://doi.org/10.1007/s11144-017-1289-5.
Gupta, A., Waghmare, U.V., Hegde, M.S., 2010. Correlation of oxygen storage capacity and structural distortion in transition-metal-, noble-metal-, and rare-earth-ion-substituted CeO2 from first principles calculation. Chem. Mater. 22, 5184–5198. https://doi.org/10.1021/cm101145d.
Habibi, N., Rezaei, M., Majidian, N., Andache, M., 2014. CH4 reforming with CO2 for syngas production over La2O3 promoted Ni catalysts supported on mesoporous nanostructured γ-Al2O3. J. Energy Chem. https://doi.org/10.1016/S2095-4956(14)60169-8.
Halabi, M.H., de Croon, M.H.J.M., van der Schaaf, J., Cobden, P.D., Schouten, J.C., 2010a. Intrinsic kinetics of low temperature catalytic methane–steam reforming and water–gas shift over Rh/CeαZr1−αO2 catalyst. Appl. Catal. A Gen. 389, 80–91. https://doi.org/10.1016/J.APCATA.2010.09.005.
Halabi, M.H., de Croon, M.H.J.M., van der Schaaf, J., Cobden, P.D., Schouten, J.C., 2010b. Low temperature catalytic methane steam reforming over ceria–zirconia supported rhodium. Appl. Catal. A Gen. 389, 68–79. https://doi.org/10.1016/J.APCATA.2010.09.004.
Han, J., Zhan, Y., Street, J., To, F., Yu, F., 2017. Natural gas reforming of carbon dioxide for syngas over Ni–Ce–Al catalysts. Int. J. Hydrogen Energy. https://doi.org/10.1016/j.ijhydene.2017.04.131.
Harshini, D., Lee, D.H., Jeong, J., Kim, Y., Nam, S.W., Ham, H.C., Han, J.H., Lim, T.-H., Yoon, C.W., 2014. Enhanced oxygen storage capacity of Ce0.65Hf0.25M0.1O2-δ (M = rare earth elements): Applications to methane steam reforming with high coking resistance. Appl. Catal. B Environ. 148–149, 415–423. https://doi.org/10.1016/J.APCATB.2013.11.022.
Harun, N., Abidin, S.Z., Osazuwa, O.U., Taufiq-Yap, Y.H., Azizan, M.T., 2018. Hydrogen production from glycerol dry reforming over Ag-promoted Ni/Al<inf>2</inf>O<inf>3</inf>. Int. J. Hydrogen Energy. https://doi.org/10.1016/j.ijhydene.2018.03.093.
Hennings, U., Reimert, R., 2008. Stability of rhodium catalysts supported on gadolinium doped ceria under steam reforming conditions. Appl. Catal. A Gen. 337, 1–9. https://doi.org/10.1016/j.apcata.2007.11.021.
Höhlein, B., von Andrian, S., Grube, T., Menzer, R., 2000. Critical assessment of power trains with fuel-cell systems and different fuels. J. Power Sources 86, 243–249. https://doi.org/10.1016/S0378-7753(99)00459-0.
Horlyck, J., Lawrey, C., Lovell, E.C., Amal, R., Scott, J., 2018. Elucidating the impact of Ni and Co loading on the selectivity of bimetallic NiCo catalysts for dry reforming of methane. Chem. Eng. J. 352, 572–580. https://doi.org/10.1016/J.CEJ.2018.07.009.
Huang, T.-J., Wang, C.-H., 2007. Methane decomposition and self de-coking over gadolinia-doped ceria-supported Ni catalysts. Chem. Eng. J. 132, 97–103. https://doi.org/10.1016/J.CEJ.2007.01.024.
Iglesias, I., Baronetti, G., Alemany, L., Mariño, F., 2019a. Insight into Ni/Ce1−xZrxO2−δ support interplay for enhanced methane steam reforming. Int. J. Hydrogen Energy 44, 3668–3680. https://doi.org/10.1016/J.IJHYDENE.2018.12.112.
Iglesias, I., Baronetti, G., Mariño, F., 2017. Ni/Ce0.95M0.05O2−d (M = Zr, Pr, La) for methane steam reforming at mild conditions. Int. J. Hydrogen Energy 42, 29735–29744. https://doi.org/10.1016/J.IJHYDENE.2017.09.176.
Iglesias, I., Forti, M., Baronetti, G., Mariño, F., 2019b. Zr-enhanced stability of ceria based supports for methane steam reforming at severe reaction conditions. Int. J. Hydrogen Energy 44, 8121–8132. https://doi.org/10.1016/J.IJHYDENE.2019.02.070.
Im, Y., Lee, J.H., Kwak, B.S., Do, J.Y., Kang, M., 2018. Effective hydrogen production from propane steam reforming using M/NiO/YSZ catalysts (M = Ru, Rh, Pd, and Ag). Catal. Today 303, 168–176. https://doi.org/10.1016/J.CATTOD.2017.08.056.
Iriondo, A., Barrio, V.L., Cambra, J.F., Arias, P.L., Guemez, M.B., Sanchez-Sanchez, M. C., Navarro, R.M., Fierro, J.L.G., 2010. Glycerol steam reforming over Ni catalysts supported on ceria and ceria-promoted alumina. Int. J. Hydrogen Energy 35, 11622–11633. https://doi.org/10.1016/j.ijhydene.2010.05.105.
Italiano, C., Luchters, N.T.J., Pino, L., Fletcher, J.V., Specchia, S., Fletcher, J.C.Q., Vita, A., 2018. High specific surface area supports for highly active Rh catalysts: Syngas production from methane at high space velocity. Int. J. Hydrogen Energy 43, 11755–11765. https://doi.org/10.1016/J.IJHYDENE.2018.01.136.
Iyer, M.V., Norcio, L.P., Kugler, E.L., Dadyburjor, D.B., 2004. Kinetic modeling for methane reforming with carbon dioxide over a mixed-metal carbide catalyst. Am. Chem. Soc. 45, 2712–2721. https://doi.org/10.1016/S0140-6701(04)91329-X.
Izquierdo, U., Barrio, V.L., Requies, J., Cambra, J.F., Güemez, M.B., Arias, P.L., 2013. Tri-reforming: A new biogas process for synthesis gas and hydrogen production. Int. J. Hydrogen Energy. https://doi.org/10.1016/j.ijhydene.2012.09.107.
Jalali, R., Nematollahi, B., Rezaei, M., Baghalha, M., 2019. Mesoporous nanostructured Ni/MgAl2O4 catalysts: Highly active and stable catalysts for syngas production in combined dry reforming and partial oxidation. Int. J.

Hydrogen Energy 44, 10427–10442. https://doi.org/10.1016/J.IJHYDENE.2018.12.186.
Jawad, A., Rezaei, F., Rownaghi, A.A., 2019. Highly efficient Pt/Mo-Fe/Ni-based Al2O3-CeO2 catalysts for dry reforming of methane. Catal. Today. https://doi.org/10.1016/J.CATTOD.2019.06.004.
Jiang, H., Li, H., Xu, H., Zhang, Y., 2007. Preparation of Ni/Mg x Ti 1 - x O catalysts and investigation on their stability in tri-reforming of methane. Fuel Process. Technol. https://doi.org/10.1016/j.fuproc.2007.05.007.
Juan-Juan, J., Román-Martínez, M.C., Illán-Gómez, M.J., 2009. Nickel catalyst activation in the carbon dioxide reforming of methane: Effect of pretreatments. Appl. Catal. A Gen. 355, 27–32. https://doi.org/10.1016/J.APCATA.2008.10.058.
Kaddeche, D., Djaidja, A., Barama, A., 2017. Partial oxidation of methane on co-precipitated Ni–Mg/Al catalysts modified with copper or iron. Int. J. Hydrogen Energy 42, 15002–15009. https://doi.org/10.1016/j.ijhydene.2017.04.281.
Kambolis, A., Matralis, H., Trovarelli, A., Papadopoulou, C., 2010. Ni/CeO2-ZrO2 catalysts for the dry reforming of methane. Appl. Catal. A Gen. 377, 16–26. https://doi.org/10.1016/J.APCATA.2010.01.013.
Kechagiopoulos, P.N., Angeli, S.D., Lemonidou, A.A., 2017. Low temperature steam reforming of methane: A combined isotopic and microkinetic study. Appl. Catal. B Environ. https://doi.org/10.1016/j.apcatb.2016.12.033.
Khajeh Talkhoncheh, S., Haghighi, M., 2015. Syngas production via dry reforming of methane over Ni-based nanocatalyst over various supports of clinoptilolite, ceria and alumina. J. Nat. Gas Sci. Eng. 23, 16–25. https://doi.org/10.1016/j.jngse.2015.01.020.
Kho, E.T., Lovell, E., Wong, R.J., Scott, J., Amal, R., 2017. Manipulating ceria-titania binary oxide features and their impact as nickel catalyst supports for low temperature steam reforming of methane. Appl. Catal. A Gen. 530, 111–124. https://doi.org/10.1016/J.APCATA.2016.11.019.
Kim, K.M., Kwak, B.S., Park, N.-K., Lee, T.J., Lee, S.T., Kang, M., 2017. Effective hydrogen production from propane steam reforming over bimetallic co-doped NiFe/Al2O3 catalyst. J. Ind. Eng. Chem. 46, 324–336. https://doi.org/10.1016/J.JIEC.2016.10.046.
Kim, P., Joo, J.B., Kim, H., Kim, W., Kim, Y., Song, I.K., Yi, J., 2005. Preparation of mesoporous Ni-alumina catalyst by one-step sol-gel method: Control of textural properties and catalytic application to the hydrodechlorination of o-dichlorobenzene. Catal. Letters 104, 181–189. https://doi.org/10.1007/s10562-005-7949-5.
Kim, S., Crandall, B.S., Lance, M.J., Cordonnier, N., Lauterbach, J., Sasmaz, E., 2019. Activity and stability of NiCe@SiO2 multi–yolk–shell nanotube catalyst for tri-reforming of methane. Appl. Catal. B Environ. 259,. https://doi.org/10.1016/J.APCATB.2019.118037 118037.
Kim, T.W., Park, J.C., Lim, T.H., Jung, H., Chun, D.H., Lee, H.T., Hong, S., Yang, J. Il, 2015. The kinetics of steam methane reforming over a Ni/γ-Al 2 O 3 catalyst for the development of small stationary reformers. Int. J. Hydrogen Energy 40, 4512–4518. https://doi.org/10.1016/j.ijhydene.2015.02.014.
Kohn, M.P., Castaldi, M.J., Farrauto, R.J., 2010. Auto-thermal and dry reforming of landfill gas over a Rh/γAl2O3 monolith catalyst. Appl. Catal. B Environ. https://doi.org/10.1016/j.apcatb.2009.10.029.
Krishna, K., Bueno-López, A., Makkee, M., Moulijn, J.A., 2007. Potential rare earth modified CeO2 catalysts for soot oxidation: I. Characterisation and catalytic activity with O2. Appl. Catal. B Environ. 75, 189–200. https://doi.org/10.1016/J.APCATB.2007.04.010.
Kumar, N., Shojaee, M., Spivey, J.J., 2015. Catalytic bi-reforming of methane: From greenhouse gases to syngas. Curr. Opin. Chem. Eng. https://doi.org/10.1016/j.coche.2015.07.003.
Kurungot, S., Yamaguchi, T., 2004. Stability improvement of Rh/γ-Al2O3 catalyst layer by ceria doping for steam reforming in an integrated catalytic membrane reactor system. Catal. Letters 92, 181–187. https://doi.org/10.1023/b:catl.0000014343.67377.98.
Kyriakou, V., Garagounis, I., Vourros, A., Vasileiou, E., Manerbino, A., Coors, W.G., Stoukides, M., 2016. Methane steam reforming at low temperatures in a BaZr0.7Ce0.2Y0.1O2.9 proton conducting membrane reactor. Appl. Catal. B Environ. 186, 1–9. https://doi.org/10.1016/J.APCATB.2015.12.039.
La Parola, V., Pantaleo, G., Deganello, F., Bal, R., Venezia, A.M., 2018. Plain and CeO 2 – Supported LaxNiOy catalysts for partial oxidation of CH 4. Catal. Today. https://doi.org/10.1016/j.cattod.2017.04.045.
Laosiripojana, N., Sangtongkitcharoen, W., Assabumrungrat, S., 2006. Catalytic steam reforming of ethane and propane over CeO2-doped Ni/Al2O3 at SOFC temperature: Improvement of resistance toward carbon formation by the redox property of doping CeO2. Fuel. https://doi.org/10.1016/j.fuel.2005.06.013.
Lee, S.H., Cho, W., Ju, W.S., Baek, Y.S., Chang, J.S., Park, S.E., 2004. Tri-reforming of CH4 using CO2 for production of synthesis gas to dimethyl ether. Stud. Surf. Sci. Catal. 153, 189–192. https://doi.org/10.1016/j.cattod.2003.10.005.
Lertwittayanon, K., Youravong, W., Lau, W.J., 2017. Enhanced catalytic performance of Ni/A-Al2O3catalyst modified with CaZrO3nanoparticles in steam-methane reforming. Int. J. Hydrogen Energy 42, 28254–28265. https://doi.org/10.1016/j.ijhydene.2017.09.030.
Li, B., Su, W., Lin, X., Wang, X., 2017a. Catalytic performance and characterization of Neodymium-containing mesoporous silica supported nickel catalysts for methane reforming to syngas. Int. J. Hydrogen Energy 42, 12197–12209. https://doi.org/10.1016/j.ijhydene.2017.03.159.
Li, X., Li, D., Tian, H., Zeng, L., Zhao, Z.-J., Gong, J., 2017b. Dry reforming of methane over Ni/La2O3 nanorod catalysts with stabilized Ni nanoparticles. Appl. Catal. B Environ. 202, 683–694. https://doi.org/10.1016/j.apcatb.2016.09.071.
Li, H., Qiu, Y., Wang, C., Huang, X., Zhao, Y., 2018. Nickel catalysts supported on ordered mesoporous SiC materials for CO2 reforming of methane. Catal. Today 317, 76–85. https://doi.org/10.1016/J.CATTOD.2018.02.038.
Li, B., Zhang, S., 2013. Methane reforming with CO2 using nickel catalysts supported on yttria-doped SBA-15 mesoporous materials via sol–gel process. Int. J. Hydrogen Energy 38, 14250–14260. https://doi.org/10.1016/J.IJHYDENE.2013.08.105.
Lima, S.M., Assaf, J.M., Peña, M.A., Fierro, J.L.G., 2006. Structural features of La1−xCexNiO3 mixed oxides and performance for the dry reforming of methane. Appl. Catal. A Gen. 311, 94–104. https://doi.org/10.1016/j.apcata.2006.06.010.
Lino, A.V.P., Colmenares Calderon, Y.N., Mastelaro, V.R., Assaf, E.M., Assaf, J.M., 2019. Syngas for Fischer-Tropsch synthesis by methane tri-reforming using nickel supported on MgAl2O4 promoted with Zr, Ce and Ce-Zr. Appl. Surf. Sci. 481, 747–760. https://doi.org/10.1016/J.APSUSC.2019.03.140.
M. Gaddalla, A., E. Sommer, M., 1989. Carbon dioxide reforming of methane on nickel catalysts. Chem. Eng. Sci. 44, 2825–2829. https://doi.org/10.1016/0009-2509(89)85092-4.
Maneerung, T., Hidajat, K., Kawi, S., 2011. LaNiO3 perovskite catalyst precursor for rapid decomposition of methane: Influence of temperature and presence of H2 in feed stream. Catal. Today 171, 24–35. https://doi.org/10.1016/j.cattod.2011.03.080.
Milberg, B., Juan, A., Irigoyen, B., 2017. Redox behavior of a low-doped Pr-CeO2(111) surface. A DFT+U study. Appl. Surf. Sci. 401, 206–217. https://doi.org/10.1016/J.APSUSC.2016.12.245.
Mirodatos, C., Praliaud, H., Primet, M., 1987. Deactivation of nickel-based catalysts during CO methanation and disproportionation. J. Catal. 107, 275–287. https://doi.org/10.1016/0021-9517(87)90294-6.
Mohd Arif, N.N., Abidin, S.Z., Osazuwa, O.U., Azizan, M.T., Taufiq-Yap, Y.H., 2019. Hydrogen production via CO2 dry reforming of glycerol over ReNi/CaO catalysts. Int. J. Hydrogen Energy 44, 20857–20871. https://doi.org/10.1016/J.IJHYDENE.2018.06.084.
Moradi, G.R., Rahmanzadeh, M., Sharifnia, S., 2010. Kinetic investigation of CO2 reforming of CH4 over La–Ni based perovskite. Chem. Eng. J. 162, 787–791. https://doi.org/10.1016/j.cej.2010.06.006.
Mosqueda, B., Toyir, J., Kaddouri, A., Gélin, P., 2009. Steam reforming of methane under water deficient conditions over gadolinium-doped ceria. Appl. Catal. B Environ. 88, 361–367. https://doi.org/10.1016/J.APCATB.2008.11.003.
Mu, J.F., Cornaglia, L.M., Cesar, D.V., Schmal, M., Lombardo, E.A., 2007. Kinetic Studies of the Dry Reforming of Methane over the Rh / La 2 O 3 - SiO 2 Catalyst 3, 7543–7549.
Múnera, J.F., Cornaglia, L.M., Cesar, D.V., Schmal, M., Lombardo, E.A., 2007b. Kinetic studies of the dry reforming of methane over the Rh/La 2O3-SiO2 catalyst. Ind. Eng. Chem. Res. 46, 7543–7549. https://doi.org/10.1021/ie061621p.
Muñoz, M., Moreno, S., Molina, R., 2013. Promoting effect of Ce and Pr in Co catalysts for hydrogen production via oxidative steam reforming of ethanol. Catal. Today. https://doi.org/10.1016/j.cattod.2013.04.037.
Naidja, A., Krishna, C.R., Butcher, T., Mahajan, D., 2003. Cool flame partial oxidation and its role in combustion and reforming of fuels for fuel cell systems. Prog. Energy Combust. Sci. 29, 155–191. https://doi.org/10.1016/S0360-1285(03)00018-2.
Nandini, A., Pant, K.K., Dhingra, S.C., 2005. K-, CeO2-, and Mn-promoted Ni/Al2O3 catalysts for stable CO2 reforming of methane. Appl. Catal. A Gen. https://doi.org/10.1016/j.apcata.2005.05.016.
Natesakhawat, S., Oktar, O., Ozkan, U.S., 2005. Effect of lanthanide promotion on catalytic performance of sol–gel Ni/Al2O3 catalysts in steam reforming of propane. J. Mol. Catal. A: Chem. 241, 133–146. https://doi.org/10.1016/J.MOLCATA.2005.07.017.
Navarro, M.V., Plou, J., López, J.M., Grasa, G., Murillo, R., 2019. Effect of oxidation-reduction cycles on steam-methane reforming kinetics over a nickel-based catalyst. Int. J. Hydrogen Energy 44, 12617–12627. https://doi.org/10.1016/J.IJHYDENE.2018.12.056.
Ni, C., Pan, L., Yuan, Z., Cao, L., Wang, S., 2014a. Study of methane autothermal reforming catalyst. J. Rare Earths 32, 184–188. https://doi.org/10.1016/S1002-0721(14)60049-1.
Noh, Y.S., Lee, K.Y., Moon, D.J., 2019. Hydrogen production by steam reforming of methane over nickel based structured catalysts supported on calcium aluminate modified SiC. Int. J. Hydrogen Energy. https://doi.org/10.1016/j.ijhydene.2019.04.287.
Ochoa, A., Barbarias, I., Artetxe, M., Gayubo, A.G., Olazar, M., Bilbao, J., Castaño, P., 2017. Deactivation dynamics of a Ni supported catalyst during the steam reforming of volatiles from waste polyethylene pyrolysis. Appl. Catal. B Environ. 209, 554–565. https://doi.org/10.1016/J.APCATB.2017.02.015.
Omoregbe, O., Danh, H.T., Abidin, S.Z., Setiabudi, H.D., Abdullah, B., Vu, K.B., Vo, D.-V. N., 2016. Influence of Lanthanide Promoters on Ni/SBA-15 Catalysts for Syngas Production by Methane Dry Reforming. Procedia Eng. 148, 1388–1395. https://doi.org/10.1016/j.proeng.2016.06.556.
Osazuwa, O.U., Cheng, C.K., 2018. Catalytic Conversion of Greenhouse Gases. Ref. Modul. Mater. Sci. Mater. Eng. https://doi.org/10.1016/B978-0-12-803581-8.11032-X.
Osazuwa, O.U., Khan, M.R., Lam, S.S., Assabumrungrat, S., Cheng, C.K., 2018. An assessment of the longevity of samarium cobalt trioxide perovskite catalyst during the conversion of greenhouse gases into syngas. J. Clean. Prod. https://doi.org/10.1016/j.jclepro.2018.03.060.
Osazuwa, O.U., Khan, M.R., Lam, S.S., Assabumrungrat, S., Cheng, C.K., 2018b. An assessment of the longevity of samarium cobalt trioxide perovskite catalyst

during the conversion of greenhouse gases into syngas. J. Clean. Prod. 185. https://doi.org/10.1016/j.jclepro.2018.03.060.
Otsuka, K., Ushiyama, T., Yamanaka, I., 1993. Partial Oxidation of Methane Using the Redox of Cerium Oxide. Chem. Lett. https://doi.org/10.1246/cl.1993.1517.
Pakhare, D., Schwartz, V., Abdelsayed, V., Haynes, D., Shekhawat, D., Poston, J., Spivey, J., 2014. Kinetic and mechanistic study of dry (CO2) reforming of methane over Rh-substituted La2Zr2O7 pyrochlores. J. Catal. 316, 78–92. https://doi.org/10.1016/j.jcat.2014.04.023.
Pakhare, D., Spivey, J., 2014. A review of dry (CO 2) reforming of methane over noble metal catalysts. Chem. Soc. Rev. 43, 7813–7837.
Patcas, F., Hönicke, D., 2005. Effect of alkali doping on catalytic properties of alumina-supported nickel oxide in the selective oxidehydrogenation of cyclohexane. Catal. Commun. 6, 23–27. https://doi.org/10.1016/J.CATCOM.2004.10.005.
Pelletier, L., Liu, D.D.S., 2007. Stable nickel catalysts with alumina-aluminum phosphate supports for partial oxidation and carbon dioxide reforming of methane. Appl. Catal. A Gen. 317, 293–298. https://doi.org/10.1016/J.APCATA.2006.10.028.
Pérez-Camacho, M.N., Abu-Dahrieh, J., Goguet, A., Sun, K., Rooney, D., 2014. Self-cleaning perovskite type catalysts for the dry reforming of methane. Chinese J. Catal. 35, 1337–1346. https://doi.org/10.1016/S1872-2067(14)60187-X.
Pino, L., Vita, A., Cipitì, F., Laganà, M., Recupero, V., 2011. Hydrogen production by methane tri-reforming process over Ni-ceria catalysts: Effect of La-doping. Appl. Catal. B Environ. https://doi.org/10.1016/j.apcatb.2011.02.027.
Pino, L., Vita, A., Laganà, M., Recupero, V., 2014. Hydrogen from biogas: Catalytic tri-reforming process with Ni/LaCeO mixed oxides. Appl. Catal. B Environ. 148–149, 91–105. https://doi.org/10.1016/J.APCATB.2013.10.043.
Poggio-Fraccari, E., Irigoyen, B., Baronetti, G., Mariño, F., 2014. Ce-Pr mixed oxides as active supports for Water-gas Shift reaction: Experimental and density functional theory characterization. Appl. Catal. A Gen. 485, 123–132. https://doi.org/10.1016/J.APCATA.2014.07.040.
Poggio-Fraccari, E., Mariño, F., Laborde, M., Baronetti, G., 2013. Copper and nickel catalysts supported on praseodymium-doped ceria (PDC) for the water-gas shift reaction. Appl. Catal. A Gen. 460–461, 15–20. https://doi.org/10.1016/J.APCATA.2013.04.013.
Postole, G., Nguyen, T.-S., Aouine, M., Gélin, P., Cardenas, L., Piccolo, L., 2015. Efficient hydrogen production from methane over iridium-doped ceria catalysts synthesized by solution combustion. Appl. Catal. B Environ. 166–167, 580–591. https://doi.org/10.1016/J.APCATB.2014.11.024.
Purnomo, A., Gallardo, S., Abella, L., Salim, C., Hinode, H., 2008. Effect of ceria loading on the carbon formation during low temperature methane steam reforming over a Ni/CeO2/ZrO2 catalyst. React. Kinet. Catal. Lett. 95, 213–220. https://doi.org/10.1007/s11144-008-5325-3.
Ramírez-Cabrera, E., Atkinson, A., Chadwick, D., 2004. Catalytic steam reforming of methane over Ce0.9Gd0.1O2−x. Appl. Catal. B Environ. 47, 127–131. https://doi.org/10.1016/J.APCATB.2003.08.008.
RAN, R., WENG, D., WU, Xiaodong, FAN, J., WANG, L., WU, Xiaodi, 2011. Structure and oxygen storage capacity of Pr-doped Ce0.26Zr0.74O2 mixed oxides. J. Rare Earths 29, 1053–1059. https://doi.org/10.1016/S1002-0721(10)60597-2.
Rathod, Vikram, Bhale, Purnanand V., 2014. Experimental Investigation on Biogas Reforming for Syngas Production over an Alumina based Nickel Catalyst. Energy Procedia 54, 236–245. https://doi.org/10.1016/j.egypro.2014.07.267.
Rivas, M.E., Fierro, J.L.G., Goldwasser, M.R., Pietri, E., Pérez-Zurita, M.J., Griboval-Constant, A., Leclercq, G., 2008. Structural features and performance of LaNi1−xRhxO3 system for the dry reforming of methane. Appl. Catal. A Gen. 344, 10–19. https://doi.org/10.1016/j.apcata.2008.03.023.
Ross, J.R.H., 2005. Natural gas reforming and CO2 mitigation. Catal. Today 100, 151–158. https://doi.org/10.1016/J.CATTOD.2005.03.044.
Ruiz, J.A.C., Passos, F.B., Bueno, J.M.C., Souza-Aguiar, E.F., Mattos, L.V., Noronha, F.B., 2008. Syngas production by autothermal reforming of methane on supported platinum catalysts. Appl. Catal. A Gen. 334, 259–267. https://doi.org/10.1016/j.apcata.2007.10.011.
Salcedo, A., Iglesias, I., Mariño, F., Irigoyen, B., 2018. Promoted methane activation on doped ceria via occupation of Pr(4f) states. Appl. Surf. Sci. 458, 397–404. https://doi.org/10.1016/J.APSUSC.2018.07.090.
Sarkar, B., Goyal, R., Pendem, C., Sasaki, T., Bal, R., 2016. Highly nanodispersed Gd-doped Ni/ZSM-5 catalyst for enhanced carbon-resistant dry reforming of methane. J. Mol. Catal. A: Chem. 424, 17–26. https://doi.org/10.1016/j.molcata.2016.08.006.
Schädel, B.T., Duisberg, M., Deutschmann, O., 2009. Steam reforming of methane, ethane, propane, butane, and natural gas over a rhodium-based catalyst. Catal. Today 142, 42–51. https://doi.org/10.1016/J.CATTOD.2009.01.008.
Sepehri, S., Rezaei, M., 2017. Ce promoting effect on the activity and coke formation of Ni catalysts supported on mesoporous nanocrystalline Γ-Al2O3 in autothermal reforming of methane. Int. J. Hydrogen Energy 42, 11130–11138. https://doi.org/10.1016/j.ijhydene.2017.01.096.
Sepehri, S., Rezaei, M., Wang, Y., Younesi, A., Arandiyan, H., 2018. The evaluation of autothermal methane reforming for hydrogen production over Ni/CeO2 catalysts. Int. J. Hydrogen Energy 43, 22340–22346. https://doi.org/10.1016/J.IJHYDENE.2018.10.016.
Shan, W., Luo, M., Ying, P., Shen, W., Li, C., 2003. Reduction property and catalytic activity of Ce1-XNiXO2 mixed oxide catalysts for CH4 oxidation. Appl. Catal. A Gen. https://doi.org/10.1016/S0926-860X(02)00659-2.
Shannon, R.D., 1976. Revised effective ionic radii and systematic studies of interatomic distances in halides and chalcogenides. Acta Crystallogr. Sect. A 32, 751–767. https://doi.org/10.1107/S0567739476001551.
Shyu, J.Z., Weber, W.H., Gandhi, H.S., 1988. Surface characterization of alumina-supported ceria. J. Phys. Chem. 92, 4964–4970. https://doi.org/10.1021/j100328a029.
Siang, T.J., Bach, L.G., Singh, S., Truong, Q.D., Ho, V.T.T., Huy Phuc, N.H., Alenazey, F., Vo, D.V.N., 2019. Methane bi-reforming over boron-doped Ni/SBA-15 catalyst: Longevity evaluation. Int. J. Hydrogen Energy 44, 20839–20850. https://doi.org/10.1016/j.ijhydene.2018.06.123.
Singh, S., Bahari, M.B., Abdullah, B., Phuong, P.T.T., Truong, Q.D., Vo, D.V.N., Adesina, A.A., 2018. Bi-reforming of methane on Ni/SBA-15 catalyst for syngas production: Influence of feed composition. Int. J. Hydrogen Energy 43, 17230–17243. https://doi.org/10.1016/j.ijhydene.2018.07.136.
Singha, R.K., Shukla, A., Yadav, A., Adak, S., Iqbal, Z., Siddiqui, N., Bal, R., 2016. Energy efficient methane tri-reforming for synthesis gas production over highly coke resistant nanocrystalline Ni-ZrO 2 catalyst. Appl. Energy. https://doi.org/10.1016/j.apenergy.2016.06.043.
Singha, R.K., Shukla, A., Yadav, A., Sivakumar Konathala, L.N., Bal, R., 2017. Effect of metal-support interaction on activity and stability of Ni-CeO2 catalyst for partial oxidation of methane. Appl. Catal. B Environ. https://doi.org/10.1016/j.apcatb.2016.09.060.
Slagtern, A., Schuurman, Y., Leclercq, C., Verykios, X., Mirodatos, C., 1997. Specific features concerning the mechanism of methane reforming by carbon dioxide over Ni/La2O3 catalyst. J. Catal. 172, 118–126. https://doi.org/10.1006/jcat.1997.1823.
Song, C., Pan, W., 2004. Tri-reforming of methane: A novel concept for catalytic production of industrially useful synthesis gas with desired H2/CO ratios. Catal. Today 98, 463–484. https://doi.org/10.1016/j.cattod.2004.09.054.
Srivastava, R., Srinivas, D., Ratnasamy, P., 2006. Sites for CO2 activation over amine-functionalized mesoporous Ti(Al)-SBA-15 catalysts. Microporous Mesoporous Mater. 90, 314–326. https://doi.org/10.1016/J.MICROMESO.2005.10.043.
Su, Y.-J., Pan, K.-L., Chang, M.-B., 2014. Modifying perovskite-type oxide catalyst LaNiO3 with Ce for carbon dioxide reforming of methane. Int. J. Hydrogen Energy 39, 4917–4925. https://doi.org/10.1016/j.ijhydene.2014.01.077.
Sutthiumporn, K., Kawi, S., 2011. Promotional effect of alkaline earth over Ni–La2O3 catalyst for CO2 reforming of CH4: Role of surface oxygen species on H2 production and carbon suppression. Int. J. Hydrogen Energy 36, 14435–14446. https://doi.org/10.1016/j.ijhydene.2011.08.022.
Sutthiumporn, K., Maneerung, T., Kathiraser, Y., Kawi, S., 2012. CO2 dry-reforming of methane over La0.8Sr0.2Ni0.8M0.2O3 perovskite (M = Bi Co, Cr, Cu, Fe): Roles of lattice oxygen on C-H activation and carbon suppression. Int. J. Hydrogen Energy 37, 11195–11207. https://doi.org/10.1016/j.ijhydene.2012.04.059.
Taherian, Z., Yousefpour, M., Tajally, M., Khoshandam, B., 2017. Catalytic performance of Samaria-promoted Ni and Co/SBA-15 catalysts for dry reforming of methane. Int. J. Hydrogen Energy 42, 24811–24822. https://doi.org/10.1016/j.ijhydene.2017.08.080.
Theofanidis, S.A., Batchu, R., Galvita, V.V., Poelman, H., Marin, G.B., 2016. Carbon gasification from Fe–Ni catalysts after methane dry reforming. Appl. Catal. B Environ. 185, 42–55. https://doi.org/10.1016/j.apcatb.2015.12.006.
Tsipouriari, V.A., Verykios, X.E., 2001. Kinetic study of the catalytic reforming of methane with carbon dioxide to synthesis gas over Ni/La2O3 catalyst. Catal. Today 64, 83–90. https://doi.org/10.1016/S0920-5861(00)00511-3.
Usman, M., Wan Daud, W.M.A., Abbas, H.F., 2015. Dry reforming of methane: Influence of process parameters—A review. Renew. Sustain. Energy Rev. 45, 710–744. https://doi.org/10.1016/j.rser.2015.02.026.
Van Santen, R.A., 2009. Complementary structure sensitive and insensitive catalytic relationships. Acc. Chem. Res. 42, 57–66. https://doi.org/10.1021/ar800022m.
Veiga, S., Romero, M., Faccio, R., Segobia, D., Duarte, H., Apesteguía, C., Bussi, J., 2019. Hydrogen-rich gas production by steam and oxidative steam reforming of crude glycerol over Ni-La-Me mixed oxide catalysts (Me= Ce and/or Zr). Catal. Today. https://doi.org/10.1016/j.cattod.2019.02.008.
Vita, A., Pino, L., Cipitì, F., Laganà, M., Recupero, V., 2014. Biogas as renewable raw material for syngas production by tri-reforming process over NiCeO2 catalysts: Optimal operative condition and effect of nickel content. Fuel Process. Technol. 127, 47–58. https://doi.org/10.1016/J.FUPROC.2014.06.014.
Walker, D.M., Pettit, S.L., Wolan, J.T., Kuhn, J.N., 2012. Synthesis gas production to desired hydrogen to carbon monoxide ratios by tri-reforming of methane using Ni-MgO-(Ce,Zr)O2 catalysts. Appl. Catal. A Gen. https://doi.org/10.1016/j.apcata.2012.08.015.
Wang, J.B., Hsiao, S.-Z., Huang, T.-J., 2003. Study of carbon dioxide reforming of methane over Ni/yttria-doped ceria and effect of thermal treatments of support on the activity behaviors. Appl. Catal. A Gen. 246, 197–211. https://doi.org/10.1016/S0926-860X(03)00054-1.
Wang, L., Liu, H., Liu, Y., Chen, Y., Yang, S., 2013. Influence of preparation method on performance of Ni-CeO2 catalysts for reverse water-gas shift reaction. J. Rare Earths. https://doi.org/10.1016/S1002-0721(12)60320-2.
Wang, N., Chu, W., Zhang, T., Zhao, X.S., 2012. Synthesis, characterization and catalytic performances of Ce-SBA-15 supported nickel catalysts for methane dry reforming to hydrogen and syngas. Int. J. Hydrogen Energy 37, 19–30. https://doi.org/10.1016/j.ijhydene.2011.03.138.
Wang, R., Xu, H., Liu, X., Ge, Q., Li, W., 2006. Role of redox couples of Rh0/Rhδ+ and Ce4+/Ce3+ in CH4/CO2 reforming over Rh-CeO2/Al2O3 catalyst. Appl. Catal. A Gen. 305, 204–210. https://doi.org/10.1016/j.apcata.2006.03.021.
Wang, S., Lu, G.Q., 1998. Role of CeO2 in Ni/CeO2-Al2O3 catalysts for carbon dioxide reforming of methane. Appl. Catal. B Environ. https://doi.org/10.1016/S0926-3373(98)00081-2.

Watanabe, F., Kaburaki, I., Shimoda, N., Satokawa, S., 2016. Influence of nitrogen impurity for steam methane reforming over noble metal catalysts. Fuel Process. Technol. https://doi.org/10.1016/j.fuproc.2016.06.003.

Wattanathana, W., Nootsuwan, N., Veranitisagul, C., Koonsaeng, N., Laosiripojana, N., Laobuthee, A., 2015. Simple cerium-triethanolamine complex: Synthesis, characterization, thermal decomposition and its application to prepare ceria support for platinum catalysts used in methane steam reforming. J. Mol. Struct. 1089, 9–15. https://doi.org/10.1016/J.MOLSTRUC.2015.02.010.

Wei, J., Iglesia, E., 2004. Structural requirements and reaction pathways in methane activation and chemical conversion catalyzed by rhodium. J. Catal. 225, 116–127. https://doi.org/10.1016/j.jcat.2003.09.030.

Whang, H.S., Choi, M.S., Lim, J., Kim, C., Heo, I., Chang, T.S., Lee, H., 2017. Enhanced activity and durability of Ru catalyst dispersed on zirconia for dry reforming of methane. Catal. Today 293–294, 122–128. https://doi.org/10.1016/j.cattod.2016.12.034.

Wrobel, G., Sohier, M.P., D'Huysser, A., Bonnelle, J.P., Marcq, J.P., 1993. Hydrogenation catalysts based on nickel and rare earth oxides: Part II: XRD, electron microscopy and XPS studies of the cerium-nickel-oxygen-hydrogen system. Appl. Catal. A Gen. 101, 73–93. https://doi.org/10.1016/0926-860X(93)80139-H.

Xu, S., Yan, X., Wang, X., 2006. Catalytic performances of NiO-CeO2 for the reforming of methane with CO2 and O2. Fuel. https://doi.org/10.1016/j.fuel.2006.03.022.

Yoo, J., Bang, Y., Han, S.J., Park, S., Song, J.H., Song, I.K., 2015. Hydrogen production by tri-reforming of methane over nickel–alumina aerogel catalyst. J. Mol. Catal. A: Chem. 410, 74–80. https://doi.org/10.1016/J.MOLCATA.2015.09.008.

Zahedinezhad, M., Rowshanzamir, S., Eikani, M., 2009. Autothermal reforming of methane to synthesis gas: Modeling and simulation. Int. J. Hydrogen Energy 34, 1292–1300. https://doi.org/10.1016/j.ijhydene.2008.11.091.

Zhang, G., Liu, J., Xu, Y., Sun, Y., 2019. Ordered mesoporous Ni/Silica-carbon as an efficient and stable catalyst for CO2 reforming of methane. Int. J. Hydrogen Energy 44, 4809–4820. https://doi.org/10.1016/J.IJHYDENE.2019.01.017.

Zhang, Z., Verykios, X.E., 1996a. Mechanistic aspects of carbon dioxide reforming of methane to synthesis gas over Ni catalysts. Catal. Letters 38, 175–179. https://doi.org/10.1007/BF00806565.

Zhang, Z., Verykios, X.E., 1996b. Carbon dioxide reforming of methane to synthesis gas over Ni/La2O3 catalysts. Appl. Catal. A Gen. 138, 109–133. https://doi.org/10.1016/0926-860X(95)00238-3.

Zhang, Z.L., Verykios, X.E., 1994. Carbon dioxide reforming of methane to synthesis gas over supported Ni catalysts. Catal. Today 21, 589–595. https://doi.org/10.1016/0920-5861(94)80183-5.

Zhao, X., Walker, D.M., Maiti, D., Petrov, A.D., Kastelic, M., Joseph, B., Kuhn, J.N., 2018. NiMg/Ceria-Zirconia Cylindrical Pellet Catalysts for Tri-reforming of Surrogate Biogas. Ind. Eng. Chem. Res. 57, 845–855. https://doi.org/10.1021/acs.iecr.7b03669.

Zhu, Yanan, Yao, Zhigang, Xu, Fan, 2018. Cationic-lanthanide-complex-catalyzed reaction of 2-hydroxychalcones with naphthols: Facile synthesis of 2,8-dioxabicyclo[3.3.1]nonanes. Tetrahedron 74 (31), 4211–4219. https://doi.org/10.1016/j.tet.2018.06.038.

Zhuang, Q., Qin*, Y., Chang, L., 1991. Promoting effect of cerium oxide in supported nickel catalyst for hydrocarbon steam-reforming. Appl. Catal. 70, 1–8. https://doi.org/10.1016/S0166-9834(00)84149-4.

Zou, H., Chen, S., Huang, J., Zhao, Z., 2016. Effect of additives on the properties of nickel molybdenum carbides for the tri-reforming of methane. Int. J. Hydrogen Energy 41, 16842–16850. https://doi.org/10.1016/J.IJHYDENE.2016.07.108.